REFRIGERATION SYSTEM BASED ON VAPOR-ABSORPTION CYCLE WITH SOLAR POWERED GENERATOR

A Final Year Project Report

Presented to

SCHOOL OF MECHANICAL & MANUFACTURING ENGINEERING

Department of Mechanical Engineering

NUST

ISLAMABAD, PAKISTAN

In Partial Fulfillment
of the Requirements for the Degree of
Bachelor of Mechanical Engineering

---

by

Muhammad Zia Ullah
Muhammad Zain Ul Abedin
Irtaza Asghar
Umer Zahid

June 2022

EXAMINATION COMMITTEE

We hereby recommend that the final year project report prepared under our supervision by:

Muhammad Zia Ullah	258186
Muhammad Zain Ul Abedin	244977
Irtaza Asghar	261946
Umer Zahid	246544

Titled: "Refrigeration System based on Vapor-Absorption Cycle with Solar Powered Generator" be accepted in partial fulfillment of the requirements for the award of Mechanical Engineering degree with grade ___

Supervisor: Engineer Abdul Naeem Khan, Assistant Professor	Dated:

_____ _____

(Head of Department) (Date)

COUNTERSIGNED

Dated: _____ _____

(Dean / Principal)

ABSTRACT

Energy is the life artery of the modern world and increasing CO_2 emission represent a beginning of life's end, so the unique way for life continuity is more research in clean and renewable energy such as solar energy. One of the needful things in the field of solar energy application is the air conditioning and refrigeration. Due to various factors like pollution and the cost of non-renewable energy sources, the world is now moving towards renewable energy sources. One of the major renewable energy sources is the sun.

Solar energy is the most abundant source of energy, but we haven't yet developed efficient technology to harness it for a variety of applications. As a result, the primary aim of this project will be to study and construct an environmentally friendly vapor absorption refrigeration system using solar energy. Evaporation, absorption, and regeneration are the three phases of the vapor absorption system, which consists of two fluids: lithium bromide and water. When the boiling point is low, refrigerants evaporate in this refrigeration system. They take some heat with them, producing a cooling effect, and they transform gas back into liquid. In this system, the compressor is replaced by a generator and an absorber.

ACKNOWLEDGMENTS

First and foremost, praise and thanks to Allah Almighty, who bestowed us with the ability and potential to work on this project. We also pay our gratitude to the Almighty for allowing us to complete this report within due course of time.

We would like to express our deep and sincere gratitude to our supervisor, Engineer Abdul Naeem Khan, Assistant Professor, National University of Science and Technology, for giving us the opportunity to do research and providing inspiring guidance throughout the project. We have been tremendously moved by his enthusiasm, vision, and motivation. He has taught us how to carry out the project and how to deliver the work in the most clear and concise manner feasible. We would also like to express our gratitude for his patience, excitement, insightful comments, important recommendations, useful information, and practical guidance during the discussion we had with him on our project.

There are very few words to express enormous, humble obligations to our affectionate parents for their prayers and strong determination to enable us to achieve this job.

ORIGINALITY REPORT

We hereby confirm that this is our original work. We have done this work on our own. If otherwise, it is mentioned with the proper reference.

TABLE OF CONTENTS

ABSTRACT ..... **ii**

ACKNOWLEDGMENTS ..... **iii**

ORIGINALITY REPORT ..... **iv**

LIST OF FIGURES ..... **viii**

ABBREVIATIONS ..... **ix**

NOMENCLATURE ..... **ix**

Subscript ..... **x**

CHAPTER 1: INTRODUCTION **11**

CHAPTER 2: LITERATURE REVIEW **13**

Introduction **13**

Refrigeration System **14**

Wilson's Plot **27**

Vacuum Vessel Design **31**

Renewable Energy **32**

Types of Solar Collectors **33**

Solar Tracking: **38**

CHAPTER 3: METHODOLOGY **41**

Refrigeration System Calculations: **41**

CAD Model: **46**

Calculations for Solar Collector: **54**

Engineering Equation Solver Software: **56**

CHAPTER 4: RESULTS and DISCUSSIONS **57**

CHAPTER 5: CONCLUSION AND RECOMMENDATION **65**

References **66**

APPENDIX I: Temperature-Pressure-concentration graph of Lithium bromide-H2O solutions [36] **71**

APPENDIX II: Temperature-Concentration-Enthalpy Graph of Lithium Bromide-H2O Solutions [37] **72**

APPENDIX IIi: Caculations **73**

Enthalpy Calculation: **73**

Condenser **76**

Evaporator **81**

Vacuum Vessel **82**

LIST OF TABLES

Table 2. 1 Comparison of Solar Collector [29] *37*

Table 3. 1 Enthalpy table *44*

Table 3. 2 Heat transfer table *45*

Table 3. 3 Comparison of solar collectors [34] *54*

Table 4. 1 Water - LiBr absorption refrigeration system calculations based on a generator temperature of 90°C and absorber at 30°C *57*

Table 4. 2 Heat addition and rejection; COP of LiBr-H_2O cycle *58*

LIST OF FIGURES

Figure 2. 1 Electricity Generation in Pakistan.....13
Figure 2. 2 Simplest vapor absorption system.....15
Figure 2. 3 Schematic of single effect absorption unit.....16
Figure 2. 4 Schematic of double effect absorption unit.....17
Figure 2. 5 Equilibrium water-vapor pressure.....18
Figure 2. 6 Water pool boiling curve [17].....26
Figure 2. 7Wilson's Plot.....30
Figure 2. 8 Parabolic Trough Collector.....35
Figure 2. 9 Linear Fresnel reflector.....35
Figure 2. 10 Parabolic dish reflector.....36
Figure 2. 11 Heliostat field collector.....37

Figure 3. 1 Methodology.....42
Figure 3. 2 Schematic of single effect.....44
Figure 3. 3 CAD Model.....46
Figure 3. 4 Top view of Generator.....47
Figure 3. 5 Generator Dish.....48
Figure 3. 6 Condenser coil.....49
Figure 3. 7 Evaporator Coil.....50
Figure 3. 8 Absorber heat exchanger.....52
Figure 3. 9 Daily variation of solar flux [35].....55

Figure 4. 1 Schematic for EES.....60
Figure 4. 2 Effect of chilled water inlet temperature at COP.....61
Figure 4. 3 Effect of desorber inlet temperature at COP.....62
Figure 4. 4 Effect of desorber temperature.....63
Figure 4. 5 Effect of inlet temperatures on heat transfer.....64

ABBREVIATIONS

VARS	Vapor Absorption Refrigeration System
VCRS	Vapor Compression Refrigeration System
LiBr	Lithium bromide salt
FPC	Flat Plate Collector
PDR	Parabolic Dish Collector
LDR	Light Dependent Resistor
PIC	Peripheral Interface Controller
COP	Coefficient of Performance
ASME	American Society of Mechanical Engineers

NOMENCLATURE

T	Temperature [^{o}C, otherwise units are mentioned]
ṁ	Mass flow rate [kg/s]
h	Enthalpy [kJ/kg]
P	Absolute pressure [kPa]
x	Concentration my mass (LiBr to H_2O)
Q̇	Heat flow rate [kW]
Φ	Solar flux [kW/m^2]
η	Solar collector efficiency
A	Surface area [m^2]
d	Diameter [m]
q	nucleate pool boiling heat flux [W/m^2]
$c1$	specific heat of liquid [J/kgK]
ΔT	excess temperature [°C or K]
Pr	Prandtl number of liquids
n	experimental constant equal to 1 for water and 1.7 for other fluids
C	surface fluid factor
μ_l	dynamic viscosity [kg/ms]
g	gravitational acceleration [m/s^2]
$g0$	force conversion factor [kgm/Ns^2]
ρ	density of vapor [kg/m^3]
σ	surface tension-liquid-vapor interface [N/m]
E	Modulus of Elasticity at design temperature [MPa]

L	Total Length [mm]
S	Stress [MPa]
t	Nominal thickness [mm]

SUBSCRIPT

g	Generator
e	Evaporator
a	Absorber
c	Condenser
r	Required
l	liquid
d	designed
allow	Allowable
sf	surface
fg	vaporization
1,2,3 - - 7	stages according to figure 3.2

CHAPTER 1: INTRODUCTION

High cooling demand causes high electrical loads in summer increasing the consumption of electricity which encourages the need to find alternative ways for cooling. The traditional air-conditioning units consume more energy and are run by CFCs which lead to the depletion of the ozone layer eventually causing global warming [1]. Given the fact that solar energy is obtainable worldwide and the maximum solar power and peak cooling load happens at once, combining cooling system with solar energy will be the solution for electricity consumption problem, as well as environmental problems, as solar cooling is environmentally friendly [2]. Solar cooling systems when compared to conventional ones have higher cost making them not very competitive in the current market however when the performance parameters are improved i.e., the size of collector, the production cost can be reduced. Further cost reduction can be achieved by installing inexpensive components.

There are two components of Global Irradiance striking the Earth's surface (i) direct beam and (ii) diffuse beam. The diffuse radiation is typically harvested in collectors that operate at the temperature below 100^{o}C whereas the beam component can be concentrated and converted to heat at high temperatures. The average global annual solar energy resource potential is around 1.6 MWh/m^2, greatly exceeding the total average energy demand per unit area [3].

Vapor Absorption Refrigeration System (VARS) works on the principle of refrigerant absorption. It falls in the category of Vapor cycles like Vapor Compression Refrigeration

System (VCRS). In contrary to VCRS, in absorption systems heat is used as an input which make these systems also known as thermal energy-driven or heat operated systems.

Ammonia-Water and LiBr-Water are most used pair of refrigerants in VARS. From V.K Bajpai's work shows the absorption system using ammonia-water as refrigerant and the COP of the system was found to be around 0.58, when used with flat plate solar collector [4]. But as more research have been made in VARS it is seen that system with LiBr-Water refrigerant performs better than the Ammonia-Water solution [5].

To provide heat energy to the generator as an input there are several ways to do so and most commonly methods are Flat Plate Solar Collector, Parabolic Solar Collector, and Evacuated Tube Type Solar Collector. A study was conducted on a VARS, powered by a parabolic solar collector, with LiBr-Water as refrigerant, 3-4^{o}C drop in cabin (evaporator) was obtained over the whole working time of system [6].

This work may have partially related points to those dealt with in other review articles, it integrates and categorizes all knowledge on solar-powered absorption chiller systems to provide a helpful reference for the study of these systems. This report deals with all the main parameter related to the single stage VARS having the cooling capacity to be used for commercial use from 0900-1700 hours in the areas of Islamabad, Pakistan as well as covering the noticeable reasons of why using this system in moderate climates.

CHAPTER 2: LITERATURE REVIEW

Introduction

Pakistan is an energy deficient country. According to the Pakistan Economic Survey 2019–20, there is a deficit of about 3000 MW. This deficiency hits its peak in summers. When everyone is using refrigeration systems powered by electricity. This need of electricity cuts short if refrigeration systems use solar energy. It will save money and make refrigeration eco-friendly.

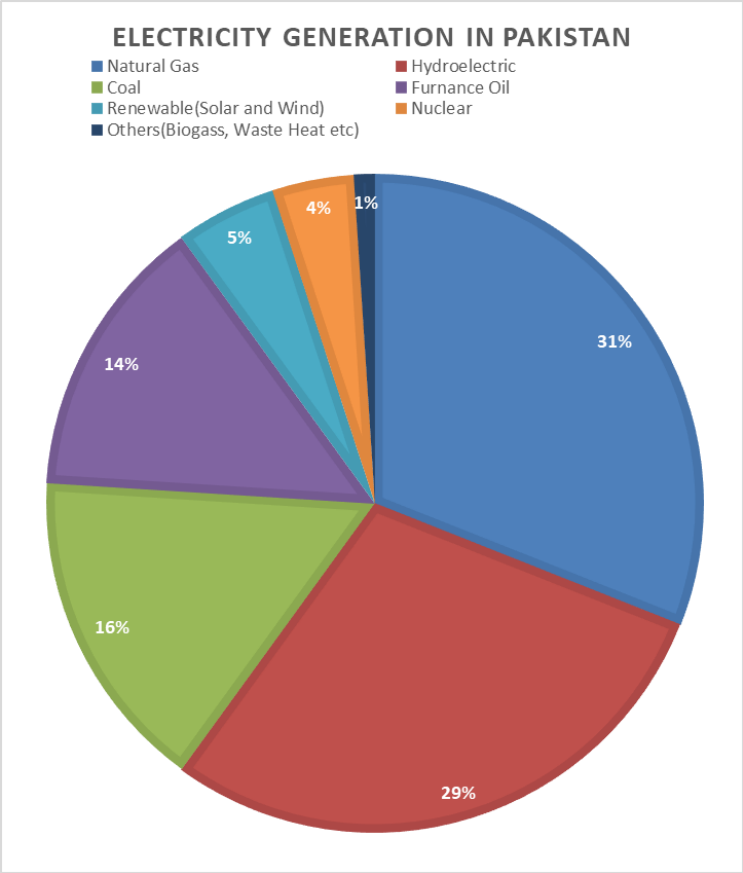

Figure 2. 1 Electricity Generation in Pakistan

Moreover, electricity generation in Pakistan is mainly about 61% using non-renewable resources like coal, natural gas, and furnace oil. These ways of producing electricity not only produce greenhouse gases but are also a source of global warming.

To solve these problems, we aim to develop a refrigeration system that does not need electricity as its main source of energy as well as it uses a renewable source of energy.

Refrigeration System

There are two major refrigeration techniques used now a days.

1. Vapor compression refrigeration system (VCRS).
2. Vapor absorption refrigeration system (VARS).

Vapor compression refrigeration system

In vapor compression refrigeration system, the input in the form of shaft work is needed to produce refrigeration. A vapor compression refrigeration system consists of a compressor, condenser, expansion valve, and an evaporator. The refrigerant after passing through the compressor becomes super-heated vapor, this super-heated vapor after condensation in the condenser passes through the expansion valve and gets evaporated in the evaporator producing cooling. A vapor compression system needs electricity to run the compressor.

Vapor absorption refrigeration system

In vapor absorption refrigeration system, the input in the form of heat is needed to produce refrigeration. It consists of a condenser and evaporator with an expansion valve

between them just like in vapor compression system and in place of compressor we have an absorber, pump, and generator. The refrigerant after being evaporated in the evaporator goes into absorber and gets absorbed. It is then pumped to the generator where refrigerant is separated from absorbent as high-pressure vapor. This super-heated vapor goes into condenser and the high concentration solution goes back into absorber via expansion valve. The super-heated refrigerant gets condensed and goes into evaporator via expansion valve producing cooling. A vapor absorption system needs heat to run generator.

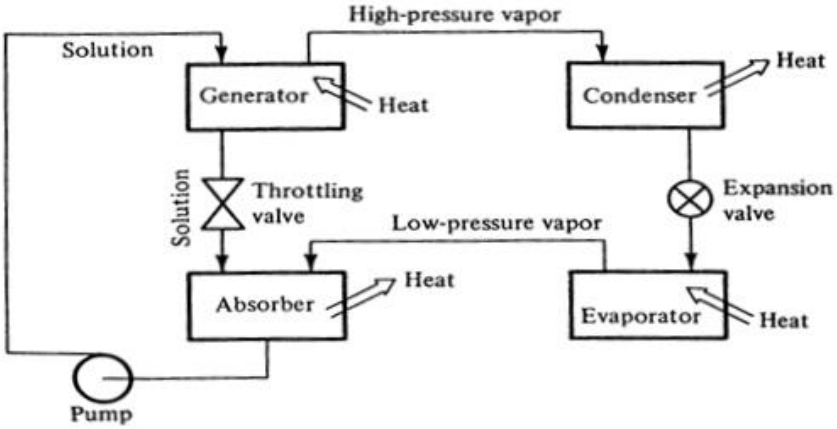

Figure 2. 2 Simplest vapor absorption system

We are going for vapor absorption system as we trying to eliminate the use of electricity from our system.

There are two common combinations of refrigerant-absorbent pairs used in air conditioning.

1. Ammonia-water combination.
2. Water-LiBr combination.

The system having water as a refrigerant and LiBr as an absorbent is more suitable for our application, and it is simpler than ammonia-water system because in water-LiBr system we do not need an analyzer and rectifier. So, we are going for water-LiBr system.

Further there are different types of water-LiBr absorption systems.

1. Single effect absorption system
2. Double effect absorption system

Single effect absorption unit

A single-effect absorption cycle using water/lithium bromide as the working fluid is perhaps the simplest manifestation of absorption heat pump technology. The schematic is shown in the figure.

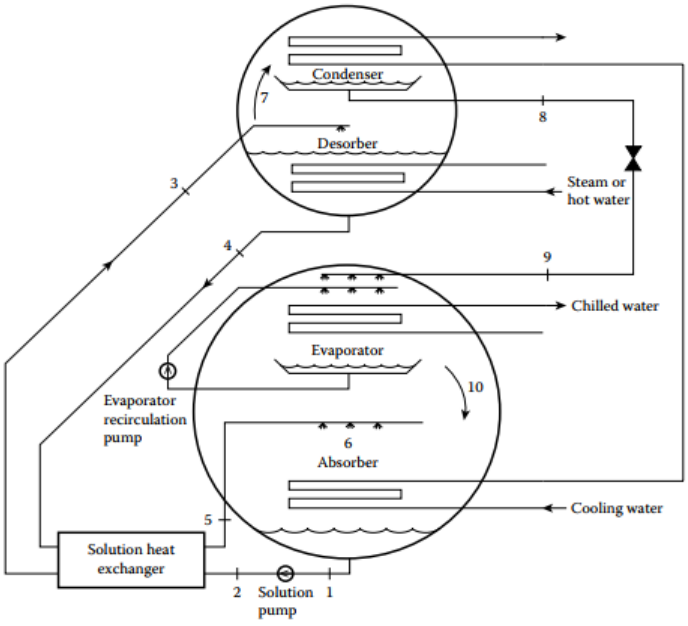

Figure 2. 3 Schematic of single effect absorption unit

Double effect absorption unit

Due to the relatively low COP associated with single-effect technology, it is difficult for single-effect machines to compete economically with conventional vapor compression systems except in high-temperature waste heat applications where the input heat energy is free. Double-effect technology, with COP in the range of 1.0–1.4, is much more competitive. The schematic is shown in figure.

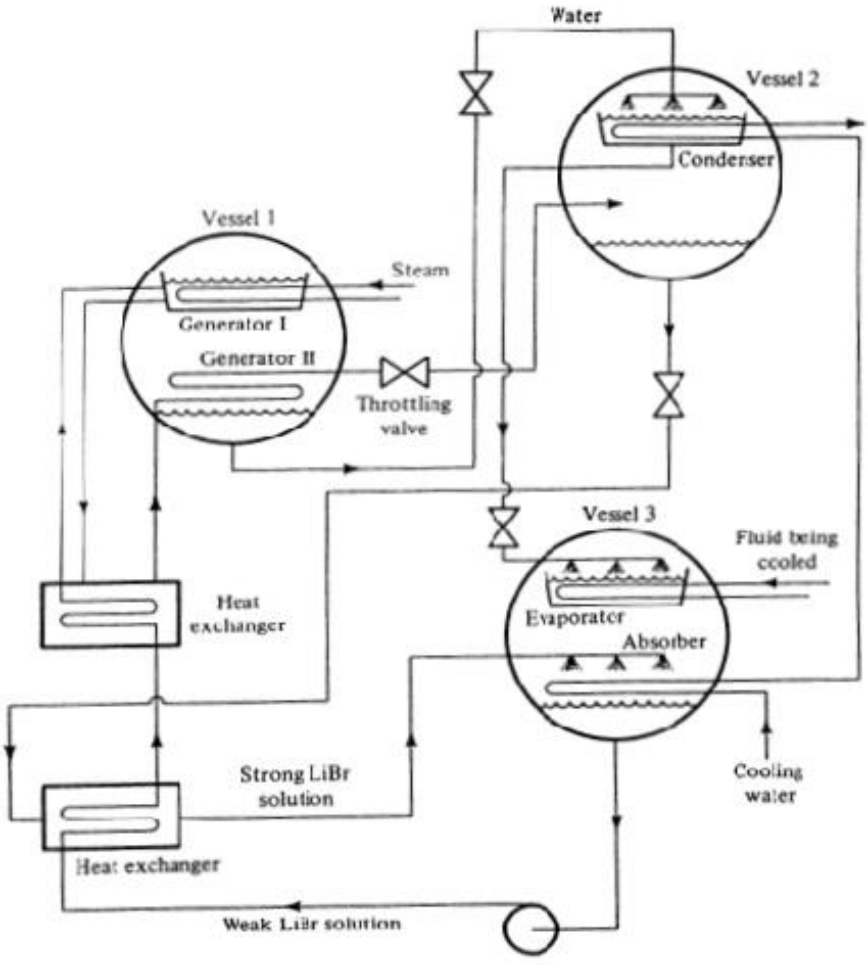

Figure 2. 4 Schematic of double effect absorption unit

Vapor Pressure of LiBr Solution

Lithium bromide is a deliquescent salt. it absorbs water vapors and become solution. Due to its hydroscopic properties, it binds the water molecules in the solution strongly than they are bound in pure water. Consequently, the vapor pressure exerted by lithium bromide solution is less than that of pure water. The figure of vapor pressure equilibrium between saturated water and lithium bromide solution is shown below. [7]

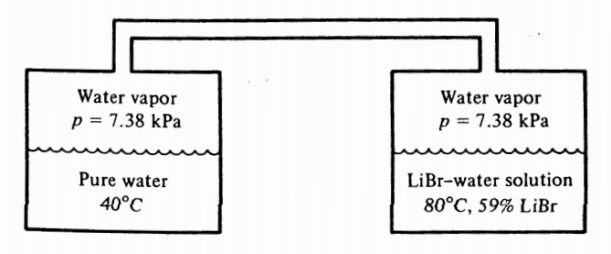

Figure 2. 5 Equilibrium water-vapor pressure

The graph between different concentration, temperature of lithium bromide solution. At 40C pure water exerts 7.38kPa vapor pressure. While lithium bromide solution of 59% concentration exerts same vapor pressure at 80C. It means if our condenser has condensed water at 40C we can know the concentration of lithium bromide in desorber as both are working at the same pressure. Similarly, if 1.23kPa pressure is exerted by pure water at 10C while lithium bromide solution with 50% concentration exerts same pressure at 30C.

Once the concentration is known, mass flow rates can be calculated by applying mass balance.

$$x_2 \dot{m}_2 = x_3 \dot{m}_3 + \dot{m}_5$$

Unknown masses are calculated. And the enthalpy can be calculated at that stage using enthalpy-concentration diagram in the appendix.

Crystallization

The main issue lithium bromide refrigeration system can face is the crystallization. If the temperature of the solution decreases below the specific value at this concentration, crystals start to form in the solution which may block the tubes and cause failure. So, system parameters are to select carefully so that crystallization does not occur. The crystallization temperature can be determined from enthalpy-concentration-temperature graph from the appendix.

Capacity Control

To control the cooling capacity of the refrigeration system, several methods are used known as capacity control. Most of the time maximum cooling is not required so system parameters have to be changed. If system is running on the same parameters while cooling load decreases, the temperature of water going to be chilled in the evaporator decreases. As a result, the vapor pressure in the evaporator decrease to a point where refrigerant will freeze and system can fail. So, it is important to reduce the performance of the system when load is decreased. Usually, temperature of chilled water leaving the evaporator is kept at constant temperature. Following methods are used to capacity control.

1. Reducing the flow rate to the generator
2. Decreasing the generator temperature
3. Increasing the condensing temperature. [8]

By these changes, other parameters also change. For example, when flow rate to generator is decreased, the flow rate of condensed refrigerant also decreases. As a result, its temperature changes which alter the vapor pressure of generator. This changes the concentration of solution leaving generator and so on. So, combination of changes is used to do capacity control.

Condenser

A condenser is a device in which a substance is condensed from gas to liquid. It is done by cooling it. The condensation occurs at constant pressure in the vapor absorption system. The refrigerant enters the condenser and changes its state from gas to liquid through the process of condensation.

There are three types of condensers

1. Water-Cooled Condenser
2. Air-Cooled Condenser
3. Evaporative Condenser

Now, we are using the water-cooled condenser for our system.

The working of the condenser consists of three phases.

1. De-superheating
2. Phase change
3. Sub-cooling

De-superheating is the process in which superheated vapors are recovered to a saturated state. Water vapors are being produced in the generator. These water vapors are at high temperatures (superheated) and pressure (pressurized). These water vapors entered the condenser. First, heat is ejected from the vapors and turned into saturated liquid.

In vapor to liquid phase change, more heat is ejected from the saturated vapor until it reaches the state where 90 percent liquid and 10 percent vapors are left.

Sub-cooling is the last phase of condensation. The sub-cooling condition is present to ensure that the liquid refrigerant does not become vapor again even if the temperature rises.

In order to design the condenser for the vapor absorption refrigeration system, we need to find the required length of the condenser. The surface area of a 1m copper tube is calculated using its diameter. Using the below formula, we need to find the area A for the required copper tube's length.

$$A = \frac{\dot{Q}}{\mathrm{U}.\Delta T}$$

We need to find out the overall coefficient U to find the required surface area.

$$U = \frac{1}{(D_0/D_i)(1/h_i) + (D_0/D_i)F_i + (1/2k)D_o \ln(D_0/D_i) + F_0 + 1/h_0}$$

Where unknown parameters are h_0 and h_i.

We can find h_0 using Nusselt No. and formula is given below:

$$h_i = \frac{N_{\mathrm{u}} \cdot k}{D_i}$$

Nusselt number can be by using Reynold number, Prandtl number and friction factor. If the value of Reynold number lies between $10^4 \leq \mathrm{Re} \leq 10^6$, then friction factor can be calculated by following relation

$$f = (0.79 \ln \mathrm{Re} - 1.64)^{-2}$$

[9]

If the value of Reynold number and Prandtl number lie between these

$$\begin{cases} 0.5 \leq \mathrm{Pr} \leq 2000 \\ 10^4 \leq \mathrm{Re} \leq 10^6 \end{cases}$$

This formula is used for finding Nusselt number for turbulent flow

$$Nu = \frac{(f/8)\mathrm{Re}\,\mathrm{Pr}}{1.07 + 12.7(f/8)^{0.5}(\mathrm{Pr}^{2/3} - 1)}$$

[10]

Once Nu is found, h_{i} can be calculated using following relation.

$$Nu = \frac{h_i D_i}{\mathrm{k}}$$

Since condensation is happening on the outside of the tube, Nusselt's relation for condensation on a horizontal surface can be used to calculate h_0. It is to be noted that the actual heat transfer coefficient can have an error of 20 percent than the heat transfer value calculated by this relation.

$$h_m = h_0 = 0.725 \left[\frac{g \rho_l (\rho_l - \rho_v) h_{\mathrm{fg}} k_l^3}{\mu_l (T_v - T_w) D_0} \right]^{0.25}$$

[11]

After finding the overall coefficient, we can find surface area. In this way, we can find the length of condenser.

Absorber

Absorber is a component in which vapors of refrigerants gets absorbed in the absorber. In lithium bromide-water system, concentrated lithium bromide solution acts as an adsorber for the water vapors coming from the evaporator.

Absorption can be done in many ways.

1. Absorption on a flat plate.
2. Absorption in a vertical flow.

Absorption is a complex phenomenon. Refrigerant and absorber are at different temperature so heat transfer occurs between them. Absorption process is usually exothermic or endothermic. Absorption of lithium bromide is and exothermic reaction. So, this heat also needs to be carried out.

During absorption, different concentration zones are created due to uneven absorption, similarly there are different temperature pools due to exothermic process. These patches are significant and we cannot take the properties at an average temperature and calculate the area required for heat transfer as it incurs significant error in calculations. Values of overall heat transfer coefficients are found experimentally [12]. Morioka conducted an

experiment for absorption in vertical piping and his overall heat transfer coefficient for absorber ranges from 1500W/m^2C to 3000W/m^2C. A practical model for absorption of vapors into a laminar film of water and LiBr falling down along a constant temperature vertical plate was described in Design Guidelines for Water-Lithium Bromide Absorbers [13]. Soteris Kalogirou made a working model of vapor absorption refrigeration system with absorber having vertical tube of steel [14]. The system has evaporator and absorber in different shells with a single passage between them. This also hinders the path of vapors to evaporator.

Generator/Desorber

In the past a lot of research work has been done on the pool boiling of different liquids yet the significant data on lithium bromide/water cannot be found [15]. Mostly values are found experimentally. They show that boiler type does not affect the boiling phenomenon but solution concentration has a major effect on the boiling. Heat transfer decreases by increase in concentration of lithium bromide. Average heat transfer coefficient of boiling varies between 1600 W/m^2°C and 7500 W/m^2°C [16]. In this study, steel tubes were used. As Rohsenow relation for boiling shows the effect of material on nucleate boiling, by using the copper tubes this heat transfer can be increased. Since there is no significant data or empirical relation for calculating heat transfer coefficient, we will be assuming the value of heat transfer coefficient which is comparable to the work done by Soteris Kalogirou.

Evaporator

Evaporator is a device which boils the refrigerant, present at low pressure, by taking the heat from the fluid. So, temperature of other fluid drops as heat is taken by the refrigerant. Evaporator has many classifications. Following classification is whether the refrigerant is present inside or outside the tubes.

1. Dry type evaporator
2. Flooded type evaporator

In dry type, refrigerant is present inside the tubes. This system is used for low cooling loads. It is compact and refrigerant vapors usually become superheated at the time of leaving. But it has low heat transfer coefficient as heat transfer is mostly occurring between gaseous refrigerants.

In flooded type, refrigerant is present outside the tubes. These evaporators are bulky and used for high cooling loads. Flooded type evaporators have high heat transfer coefficients. Recirculation of refrigerant is used for better results.

The pressure drop in the evaporator has very significant effect on the cooling capacity. If pressure drop of refrigerant in the evaporator has a significant value, COP can drop by 20-40%. So usually, flooded type evaporators are used in lithium bromide system as this design allows the vapors to freely moves towards absorber and pressure drop does not occur.

In dry type evaporator, flow boiling takes places. As the refrigerant moves inside the tubes it converts into vapors. This result in heat transfer with refrigerant vapors too which reduces the heat transfer coefficient. However, in flooded type evaporator the bool boiling takes place. In lithium bromide-water system, water is a refrigerant. So, the pool boiling curve of water is shown below:

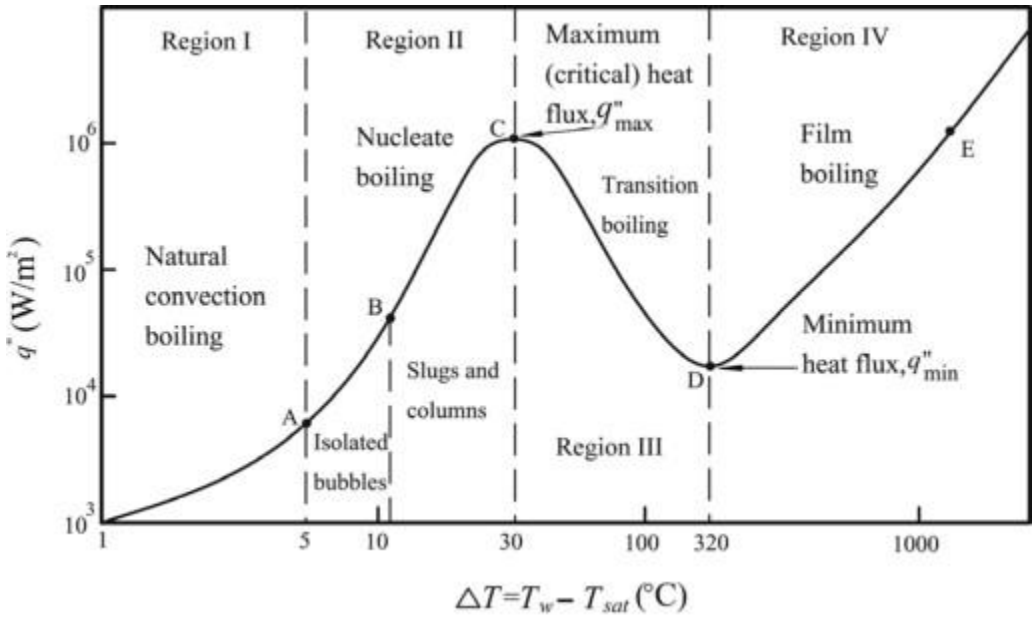

Figure 2. 6 Water pool boiling curve [17]

In our design, the chilled water has temperature difference of more the 10C than the refrigerant so nucleate boiling takes place in the evaporator. Rohsenow's correlation is used to calculate the flux for nucleate boiling of water.

$$\dot{q} = \mu_l h_{fg} \left[\frac{g(\rho_l - \rho_v)}{\sigma}\right]^{1/2} \left[\frac{C_p(T_s - T_{\text{sat}})}{C_{sf} h_{\text{fg}} Pr_l^n}\right]^3$$

[18]

The properties are calculated at average temperature of refrigerant and chilled water and heat flux is calculated.

Effect of Pressure on Evaporation

Vapor pressure affects boiling. If evaporator is designed to give chilled water at 10C, the vapor pressure should be maintained at 1.23kPa which is the saturated pressure at 10C for water. This is also the main reason; flooded type evaporator is chosen. Refrigerant is sprayed on the tubes of evaporator. If evaporator coils are submerged in water, the boiling occurs at high temperature which subsequently increases the temperature of chilled water coming out of evaporator. For the coil dipped in 1cm depth of water refrigerant, the pressure increases by 98.1 kPa. This changes the boiling point from 10C to 120C. So, boiling does not happen and heat transfer coefficient decreases significantly.

Wilson's Plot

Most convective heat transfer processes in heat exchangers have complex geometries and complicated flows, making analytical solutions impossible. As a result, a method based on Newton's rule of cooling, gives a simple solution.

$$q = h \,.\, A \,(\, T_s - \, T_f)$$

The main challenge with this technology is measuring the surface temperature because the surface temperature changes from location to location, and the presence of temperature sensors could affect the flow pattern. As a result, any alternative approach

for calculating convection coefficients in heat exchangers for heat transfer should be used due to its extensive use and practical implementation.

In several convective heat transport processes, the Wilson plot method is a useful approach for predicting convection coefficients. The Wilson plot method eliminates direct surface temperature measurement and, as a result, the disruption of fluid flow and heat transfer that occurs while trying to determine such temperatures.

The Wilson plot method deals with the determination of convection coefficients based on measured experimental data and the subsequent construction of appropriate correlation equations.

This method is derived to determine the heat transfer coefficient for which the thermal resistance on one side of the heat transfer surface remains same while changing the mass flow on the other side changes the total thermal resistance in the heat exchanger.

The main objective of this method is to determine the convection coefficient of the fluid. The modification of the Wilson plot method is to enhance the accuracy of results.

The overall thermal resistance of the process in a shell and tube heat exchanger is

$$R_{ov} = R_i + R_s + R_o$$

If mass flow rate of cooling water inside the tube changes, the change in overall thermal resistance is mainly due to R_i while remaining thermal resistance remain constant.

For turbulent flow, Nusselt equation becomes,

$$N_{\mathrm{u}} = 0.023\ (Re)^{0.8}\ (Pr)^{0.33}\ (\frac{\mu}{\mu_w})^{0.14}$$

[19]

While remaining variables are constant, Nusselt's number is proportional to Reynold number.

$$N_{\mathrm{u}}\ \propto\ (Re)^{0.8}$$

$$\frac{\mathrm{h}_i\ .\ \mathrm{D}}{k}\ \propto\ (\frac{v\ .\ D\ .\ \rho}{\mu})^{0.8}$$

$$\mathrm{h}_i\ \propto\ (v)^{0.8}$$

$$\mathrm{h}_i = C_2\ (v)^{0.8}$$

$$R_{ov} = \frac{1}{U} = \frac{1}{\mathrm{A}.\ \mathrm{h}_i} + \frac{x_w}{k} + \frac{1}{A.h_o}$$

$$R_{ov} = \frac{1}{U} = \frac{1}{C_1 A\ (v)^{0.8}} + \frac{x_w}{k} + \frac{1}{A.h_o}$$

$$C_1 = \frac{x_w}{k.A} + \frac{1}{A.h_o}$$

$$R_{ov} = \frac{1}{U} = \frac{1}{C_2\ A(v)^{0.8}} + C_1$$

This equation is analogues to the equation of straight line, having slope of $\frac{1}{C_2\ A}$ and y-intercept of C_1.

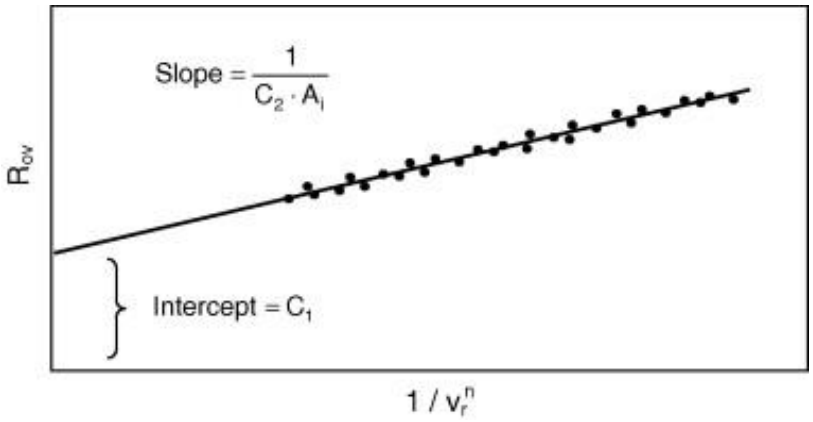

Figure 2. 7 Wilson's Plot

Simple linear regression can be used to find the straight-line equation that best fits the experimental data. It's possible that the overall thermal resistance is a function of the total amount of heat transferred coefficient and surface area.

The overall thermal resistance and the cooling liquid velocity can be obtained by experimentally measuring:

- inlet temperature
- outlet temperature
- vapor temperature at various mass flow rates under fully developed turbulent flow.

$$R_{ov} = \frac{LMTD}{m \,.\, c_p \,.\, (T_{out} - T_{in})}$$

Simple linear regression can be used to obtain the straight-line equation that best fits the experimental data. The values of the constants C1 and C2 are then calculated as shown in

the diagram above. The external and internal convection coefficients for a particular mass flow rate can be calculated once the constants C1 and C2 have been obtained.

$$h_o = \frac{1}{(C_1 - R_w)A_0}$$

[20]

It is very difficult to calculate the heat transfer coefficient for absorber and generator as discussed before. We assumed the values of heat transfer coefficients considering the previously done work on these systems. After fabrication of system, we can use Wilson plot to prove the values of heat transfer coefficients experimentally. This is an easier approach to do so.

Vacuum Vessel Design

American Society of Mechanical Engineering has set the standard for the selection criteria and process for the vacuum vessel. Section 8, division 1 has method for the selection of vacuum vessel. Every vacuum vessel is designed for full vacuum condition. The design process starts by selecting the dimensions and material of vessel. Length, diameter and selected thickness gives the factor A from ASME Sec. II subpart 3 Figure G. The value of elastic modulus for selected material at the working temperature is taken from figure HA-3 (HA is for cast iron). Then elastic modulus and factor A are used to find factor B from figure CS-1.

And maximum external pressure can be calculated from following relation

$$P_a = \frac{4B}{3(\frac{D_o}{t})}$$

[21]

Renewable Energy

Renewable energy is energy that is collected from renewable resources that are naturally replenished on human timescale. It includes sources as sunlight, wind, rain, tides, waves, and geothermal heat. Renewable energy stands in contrast to fossil fuels, which are being used far more quickly than they are being replenished. Although most renewable energy sources are sustainable, some are not. For example, some biomass sources are considered unsustainable at current rates of exploitation [22].

Out of all the renewable sources of energy we are going to opt for solar energy because it is the most abundant form of energy.

Solar Energy

Almost all the renewable energy sources originate entirely from the sun. Solar energy is a very large, inexhaustible source of energy. The power from the sun intercepted by the earth is approximately 1.8x1011 MW which is much larger than the present consumption rate on the earth of all commercial energy sources. Thus, in principle, solar energy could supply all the present and future energy needs of the world on the continuing basis. This makes it one of the most promising of the unconventional energy sources.

There are two ways to use solar energy.

1. Converting solar energy into electrical energy using solar panels.
2. Converting solar energy into thermal energy using solar collectors.

Solar Collectors

Solar energy collectors are special kinds of heat exchangers that transform solar radiation energy to internal energy of the transport medium. The major component of any solar system is the solar collector. This is a device that absorbs the incoming solar radiation, converts it into heat, and transfers the heat to a fluid (usually air, water, or oil) flowing through the collector. The solar energy collected is carried from the circulating fluid either directly to the hot water or space conditioning equipment or to a thermal energy storage tank, from which it can be drawn for use at night or on cloudy days .

There are basically two types of solar collectors.

1. Stationary collectors.
2. Sun tracking collectors.

The stationary solar collectors are permanently fixed in position and do not track the sun. They are cheap and simple and are suitable for low temperature applications like room heating [23]. Three main types of collectors fall into this category.

1. Flat-plate collector (FPC).
2. Stationary compound parabolic collector (CPC).
3. Evacuated tube collector (ETC).

Types of Solar Collectors

Energy delivery temperatures can be increased by decreasing the area from which the heat losses occur. Temperatures far above those attainable by FPCs can be reached if a

large amount of solar radiation is concentrated on a relatively small collection area. This is done by interposing an optical device between the source of radiation and the energy-absorbing surface. Following are the main types of sun tracking collectors [24].

1. Parabolic trough collector (PTC).
2. Linear Fresnel reflector (LFR).
3. Parabolic dish reflector (PDR).
4. Heliostat field collector (HFC).

The detail of them is given:

Parabolic trough collector

To deliver high temperatures with good efficiency a high-performance solar collector is required. Systems with light structures and low-cost technology for process heat applications up to 400^{o}C could be obtained with PTCs. PTCs can effectively produce heat at temperatures between 50 and 400^{o}C. Parabolic trough collectors are made by bending a sheet of reflective material into a parabolic shape. A black metal tube, covered with a glass tube to reduce heat losses, is placed along the focal line of the receiver [25].

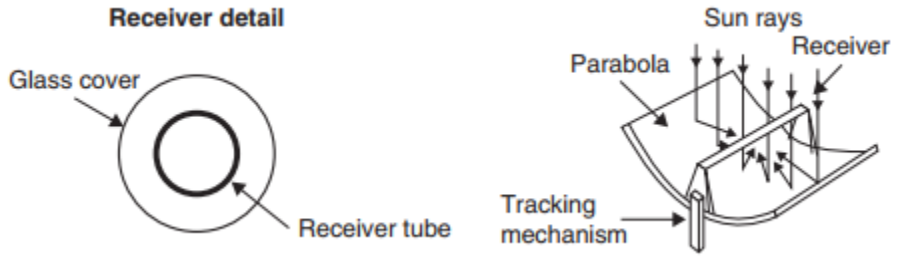

Figure 2. 8 Parabolic Trough Collector

Linear Fresnel reflector

Fresnel collectors have two variations: the Fresnel lens collector (FLC), shown in Figure (a), and the linear Fresnel reflector (LFR), shown in Figure (b). The former is made from a plastic material and shaped in the way shown to focus the solar rays to a point receiver, whereas the latter relies on an array of linear mirror strips that concentrate light onto a linear receiver [26].

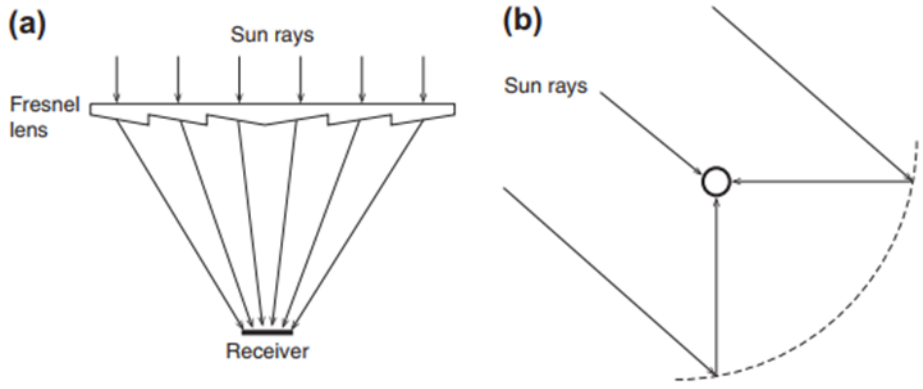

Figure 2. 9 Linear Fresnel reflector

Parabolic dish reflector

A parabolic dish reflector (PDR), shown in Figure, is a point-focus collector that tracks the sun in two axes, concentrating solar energy onto a receiver located at the focal point

of the dish. The dish structure must fully track the sun to reflect the beam into the thermal receiver. For this purpose, tracking mechanisms like the ones described in the previous section are employed in double, so the collector is tracked in two axes [27].

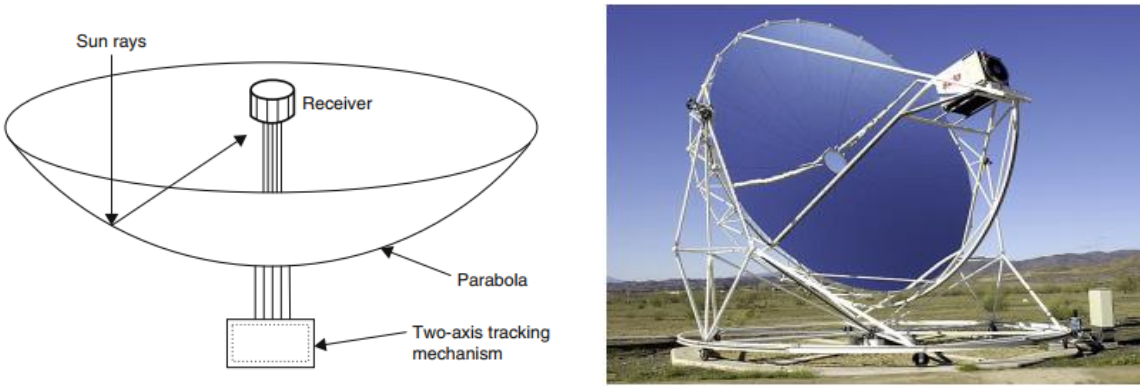

Figure 2. 10 Parabolic dish reflector

Heliostat field collector

For extremely high inputs of radiant energy, a multiplicity of flat mirrors, or heliostats, using altazimuth mounts can be used to reflect their incident direct solar radiation onto a common target, as shown in Figure. This is called the heliostat field or central receiver collector [28].

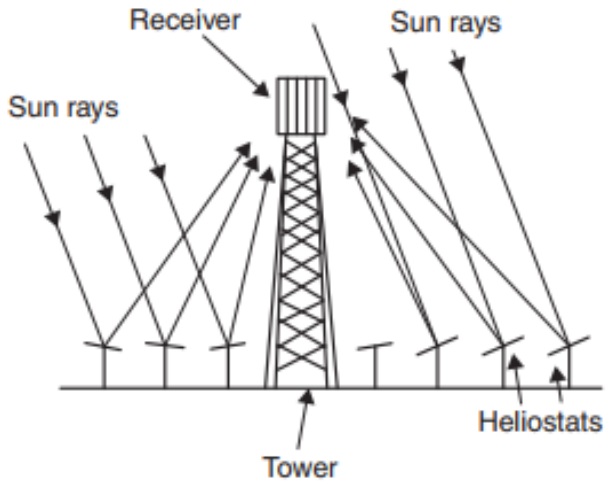

Figure 2. 11 Heliostat field collector

Comparison of solar collectors

Table 2. 1 Comparison of Solar Collector [29]

Collector Type	Absorber Type	Concentration Ratio	Indicative Temperature Range (°C)
Flat-plate collector (FPC)	Flat	1	30–80
Evacuated tube collector (ETC)	Flat	1	50–200
Compound parabolic collector (CPC)	Tubular	1–5	60–240
Compound parabolic collector (CPC)	Tubular	5–15	60–300
Linear Fresnel reflector (LFR)	Tubular	10–40	60–250
Cylindrical trough collector (CTC)	Tubular	15–50	60–300
Parabolic trough collector (PTC)	Tubular	10–85	60–400
Parabolic dish reflector (PDR)	Point	600–2000	100–1500
Heliostat field collector (HFC)	Point	300–1500	150–2000

After studying every solar collector, we are going to opt for parabolic dish reflector because it fulfills our requirement of input temperature, and it has high efficiency.

Solar Tracking:

Since we are going to use solar energy as a source of heat for our generator. The amount of heat gained from the sun depends basically upon the amount of solar energy captured by the collectors, and thereby, the necessity of design and development in solar tracking systems should be capable to follow the sun trajectory during the day on a year-round basis and that gets strong attention from the energy community. Solar energy is not constant at any direction during a day because of sun movement, whereas solar power generation system uses specific sun tracking system and that makes the available energy higher compared to the standard stable systems. One way to increase the efficiency of a solar energy dish is to manufacture the dish system by using different effective materials. The second way is to track the sun by using an efficient and fast-respond solar tracker.

Solar power generation by using a controllable moving dish is an efficient solution. When Earth is rotating, solar radiation reaching at the collectors cannot be constant at any direction in the entire day. Therefore, tracking the solar energy in each direction increases the efficiency of the system. Indeed, a solar tracker is an automated solar panel, which assists to get maximum radiation for entire day.

In this regard, dual axis tracking system is the best choice for tracking in both azimuth and altitude directions. The designed two-axis sun tracking system is distinguished by a reasonable simple and low-cost electromechanical system with low maintenance

requirement, easy-installation, and operational aspects. Besides, the hardware and software of the tracker do not require any refreshment, when a seasonal change occurs for the position of Sun.

The advantage of a dual axis solar tracking system is that Sun changes its position in the sky due to the rotation of Earth in daily basis and it even becomes more complicated in a seasonal. By the help of a dual axis solar tracking system, one can improve the efficiency of the solar power as will be pointed out. Dual axis solar tracking system especially works well, even if the weather becomes cloudy, when it is compared to the single axis solar tracking system. Among the tracker tools, single axis trackers have a disadvantage, because the location of Sun changes in the sky with a change in altitude angle, seasonally as well as with azimuth angle during the day. However, such a system only follows daily direction.

The sun tracking system that lets Parabolic Dish orthogonal to the sun radiation during the day, can raise the concentrated sun radiation by up to 30% to 40% [30]. The fixed Parabolic Dish cannot generally track the sun trajectory, also the single-axis tracking system can follow the sun in the horizontal direction (azimuth angle), while the two-axis tracker tracks the sun path in both azimuth and altitude angles. Dual axis automated control tracking system, which tracks the sun in two planes (azimuth and altitude) to move a Concentrated Parabolic Dish system to the direction of ray diffusion of sun radiation.

Some of solar tracking system conducted by other researchers uses various types of sensors including light dependent resistor (LDR) which is not efficient and can be easily affected by external environmental factors. The usage of pyranometer for measuring solar radiation as one of the input parameters. The solar tracking system controlled by PIC microcontroller that collects multiple input parameters and uses developed algorithm to control stepper motor movement. This work utilizes pyranometer sensor to sense solar radiation and PIC microcontroller act as the system brain. An algorithm developed to control the stepper motor which moves the parabolic dish. The use of sensor to track the solar position for better efficiency of solar panel [31]. However, pyranometer sensor is used to track the solar beam radiation rather than other type of sensors for this work. This is due to the properties of a pyranometer which sense the solar beam radiation. During a cloudy day, other sensor may fail to locate the position of sun efficiently as they sense light or image but pyranometer will detect the radiation therefore can maintain the power produced at maximum [32].

CHAPTER 3: METHODOLOGY

Refrigeration System Calculations:

We are designing a refrigeration system for 1 ton cooling capacity. Since our idea can be commercialized and used in different places like offices, schools, and homes for different cooling capacity. We are just generalizing the cooling capacity to 1 ton. This system can be redesigned for required load and using load calculations.

Since we know our cooling load, we next move towards selecting source of heat energy. The next selection was between solar photocell and solar collector. In solar photocell, first solar energy is converted into electrical energy and then into heat energy for our cycle. it is not suitable solution for our problem because solar photocells are not very efficient. They are 15-20% efficient while solar collectors are 60-90% efficient. And another advantage of using solar collector is that they directly convert solar energy to heat energy by concentrating it. This reduces the energy loses during conversion. So, we need smaller size solar collector than solar photocell for same energy requirement. Since we are going with solar collector. Further specific type of solar is discussed after cycle calculations. All the cycle calculations are based on book “Chapter 17, Refrigeration and Air Conditioning, Second Edition, W.F. Stoecker, J.W. Jones”. The book can be used for reference [33].

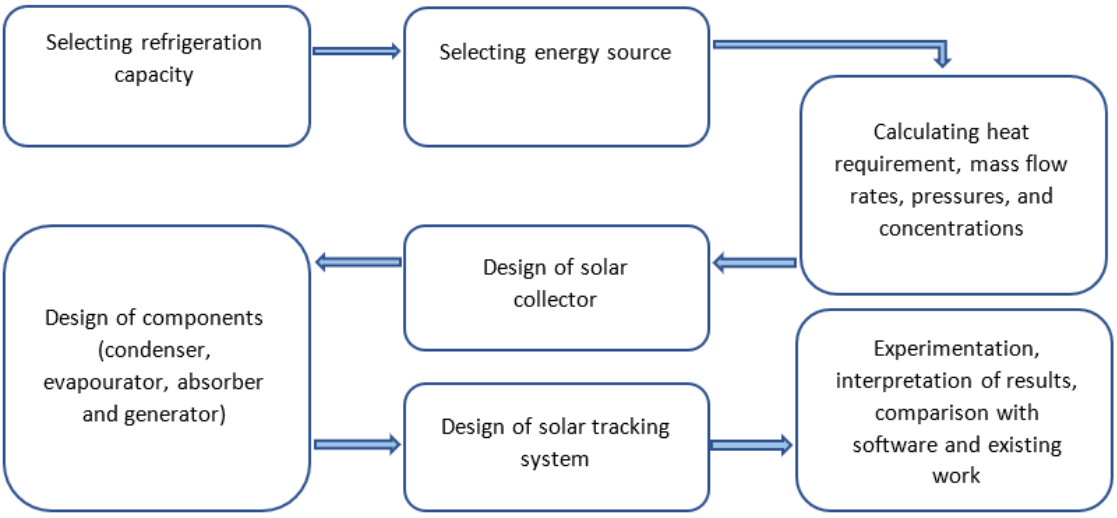

Figure 3. 1 Methodology

Now, we selected the temperatures for each component and calculated the enthalpies, pressures, concentrations, and mass flow rates according to them.

The temperatures that we are selecting for our system are given below:

Generator temperature $T_g = 90^oC$

Condenser temperature $T_c = 40^oC$

Absorber temperature $T_a = 30^oC$

Evaporator temperature $T_e = 10^oC$

These temperatures are selected carefully after iterations. The proper working of cycle lies in the value of these temperatures. If we change the condenser temperature, for example, it will change the vapor pressure of condenser which ultimately changes the pressure of generator as both are placed in same closed vessel. When pressure of generator changes, the vapor pressure of LiBr solution changes as concentration of LiBr-

H_2O solution is a function of concentration and temperature of the solution. Similarly, the evaporator temperature is influencing the pressure of absorber and consequently concentration of solution in absorber. This change in concentrations changes the mass flow rates which can vary refrigeration capacity of the system. So, we selected the condenser temperature 40^oC which means our generator and condenser are working on pressure of 7.38kPa. And evaporator temperature of 10^oC indicates the pressure of evaporator and absorber equal to 1.23kPa.

With these temperatures, we can calculate the maximum possible COP for our cycle. It is given below:

$$COP = \frac{T_g - T_a}{T_g} * \frac{T_e}{T_c - T_e}$$

$$COP = \frac{363 - 303}{363} * \frac{283}{313 - 283}$$

$$COP = 1.55$$

This is the maximum possible COP on which our system can run on selected temperatures. But in real life, actual COP is always less than 1.55 due to irreversibility's occur in the processes. Generally, actual COP is usually half of ideal COP.

Our condenser and evaporator temperatures are 40^oC and 30^oC respectively. One may argue that we can increase the COP of system by reducing the absorber and condenser temperatures. It is quite right to increase COP by reducing these temperatures but by reducing these temperatures our system is prone to have crystallization of LiBr. This will

cause blockage and system failure. So, we are going for previously discussed temperatures to avoid the risk of crystallization.

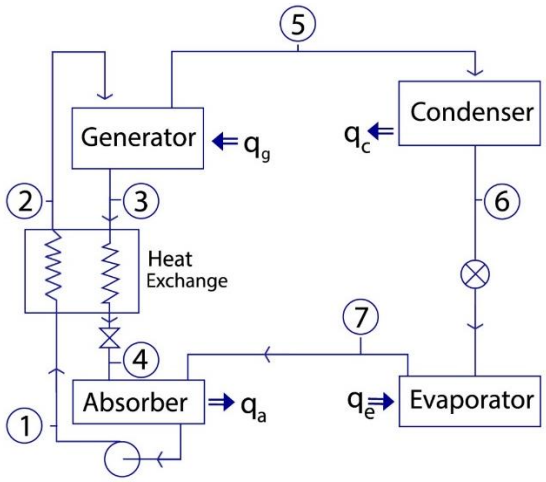

Figure 3. 2 Schematic of single effect

The table below shows the properties at each point shown in the above Diagram.

Table 3. 1 Enthalpy table

Point	h (kJ/Kg)	ṁ (kg/s)	P (kPa)	T (^oC)	%LiBr (x)	Remarks
1	-168	0.006985	7.38	30	49	Weak solution at 30^oC
2	-120.84	0.006985	7.38	50	49	Weak solution at 50 ^oC
3	-68	0.005485	7.38	90	62.4	Rich solution at 90 ^oC
4	-128	0.005485	1.23	60	62.4	Rich solution at 60 ^oC
5	2659.5	0.0015	7.38	90	0	Saturated water vapors at 90 ^oC
6	167.53	0.0015	7.38	40	0	Saturated water liquid at 40 ^oC
7	2519.2	0.0015	1.23	10	0	Saturated water vapors at 10 ^oC

The table above shows the enthalpy, mass flow rate, absolute pressure, temperature in each component, concentration of Li-Br Solution, and finally the state of the solution in each component which gives us the idea of how our system is working on different parameters and giving us the desired output.

Further moving on to the discussion of heat transfer in each component of our Absorption System that includes our generator, condenser, evaporator and finally absorber. The table below shows the heat transfer in every component of our system.

The equation used for finding the heat transfer for every component in our system is as:

$$\dot{Q} = \dot{m}\,(h_o - h_i)$$

The table below shows the heat transfer in each component of our Absorption system.

Table 3. 2 Heat transfer table

Description	Symbol	kW
Cooling Capacity	$\dot{Q}_e$	3.5
Absorber Heat (Rejected to Environment)	$\dot{Q}_a$	4.25
Heat input to the Generator	$\dot{Q}_g$	4.46
Condenser Heat (Rejected to the Environment)	$\dot{Q}_c$	3.7
Coefficient of Performance	COP	**0.78**

Note that the Theoretical COP of our system is calculated as:

$$COP = \frac{Q_e}{Q_g} = \frac{3.5\ kW}{4.46\ kW} = 0.78$$

Now we can see that COP drops from 1.55 to 0.78 for actual cycle. Even though we did not include any heat loss, considered ideal stages and complete heat transfer. So, by

taking these parameters into consideration, practical COP of the system should be expected to lower than 0.78.

Since above the heat transfer through each component is calculated, now to achieve that heat transfer each component must be designed accordingly inside our pressure vessels. The Design of each component is discussed as below.

CAD Model:

The cad model of our system is shown below. Above cylinder has coiled shape condenser and long bar shaped desorber. While below cylinder has coiled shape evaporator and bar shape absorber.

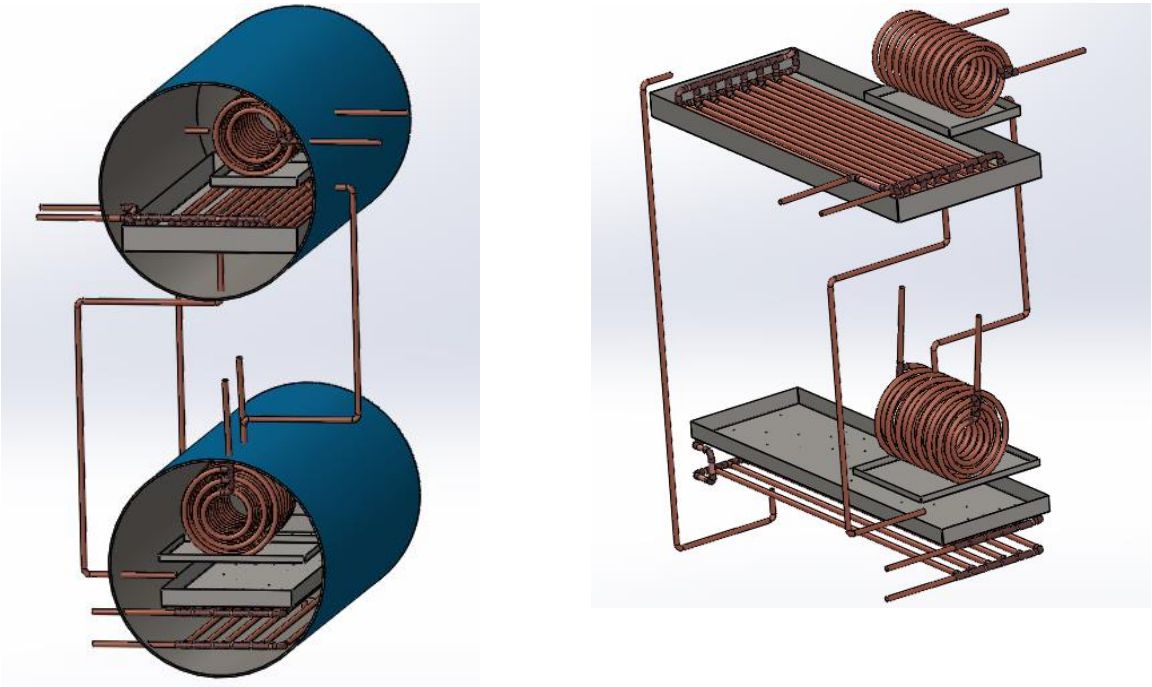

Figure 3. 3 CAD Model

Generator:

The diagram of our generator is as shown:

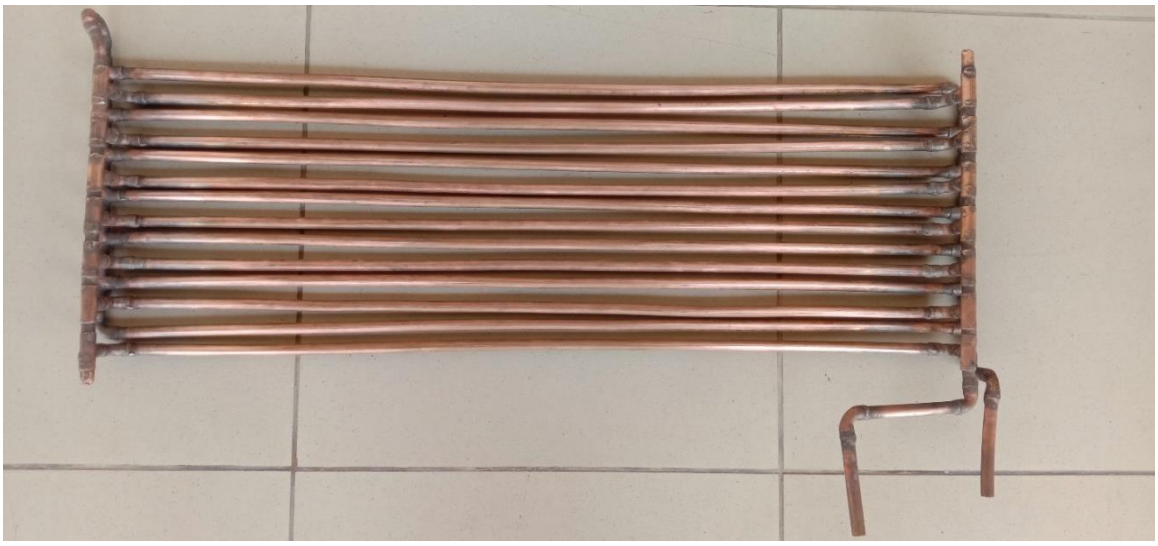

Figure 3. 4 Top view of Generator

Figure shows the top view of our generator as we can see that the length calculated to achieve the heat transfer of 4.46kW through the generator is 10m, calculations for this are shown in the appendix of the report. Note that the hot water at the temperature of $95^{o}C$ will enter the tubes of copper having the diameter of $3/8''$ (inches) and by moving from each tube it will exit at the temp of $90^{o}C$, and the change of 5 degrees will be transferred to the Li-Br Solution present in the generator dish will absorb that heat and high pressure water vapors are generated which then strikes the condenser coils which will be discussed further on. Figure attached shows the complete picture of the generator dish with the copper tubes inside them.

Figure 3. 5 Generator Dish

Note that the volume of the generator dish is of maximum 7-liters but for our operations we only need about 3Liters of Li-Br water solution inside the dish to further carry on our operations in condenser. Note that the material used for making dish is galvanized sheet metal having gauge of 25 i.e., thickness in inches is 7/320. Note that all the cooper tubes are fully submerged in the Li-Br solution.

There is a hole at the right side of the generator dish which will allow the concentrated Li-Br to move down, under the force of gravity and will be moved down on the absorber sheet which will be discussed later.

Condenser

For designing our condenser, we firstly focused on having vertical tube condenser just like in automobiles because vertical tube condensers gives more space to the coming condensate and more tube gets in-contact with the falling condensate but in our case the main issue faced was space constraint, as we must place not only our generator but also

the condenser inside a 380mm diameter pressure vessel having gauge of 10 which is 3.25mm. So, we went with the approach to not have vertical and horizontal tube condenser, thus giving us the shape of coil as shown as:

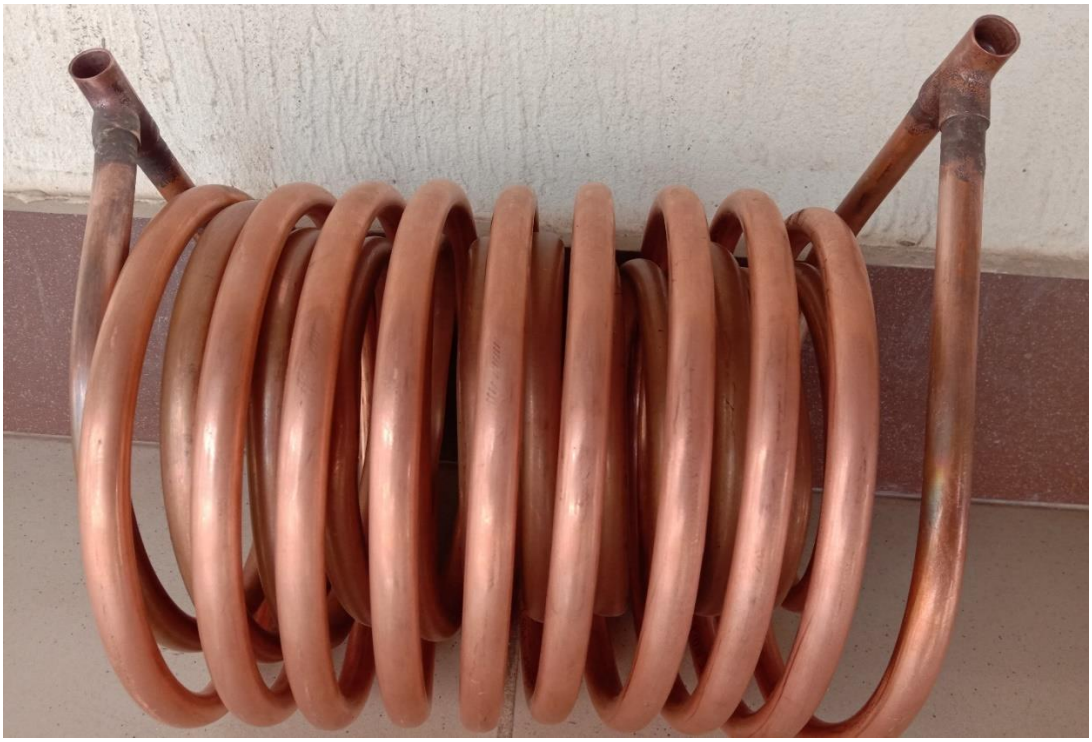

Figure 3. 6 Condenser coil

Note that the outside diameter of the coils present inside the coil type condenser are 101.6mm and 137.9mm. The heat transfer through the condenser as calculated above is 3.7kW and the length calculated to get this heat transfer rejected to the environment is 6m. As stated above vertical type condenser of length of 6m couldn't be placed inside a 380mm diameter pressure vessel so to get the stated heat transfer we make a mix type condenser having both horizontal and vertical tubes.

Now the water vapors generated by the “Generator coils” will strike with the condenser coils and water flowing inside the coils with gain the heat of those water vapors result in the condensation of the water vapors inside the pressure vessels, which will be collected at the bottom of the 1st pressure vessel and using a copper tube with will be transferred to the 2nd pressure vessel present below the first one, which will then strike the absorber coils and will gain heat from the water flowing inside the tubes and thus cooling effect will be generated at the outlet of the absorber coils which will be discussed in the coming definition.

Evaporator

The next component in our refrigeration system is evaporator which is present in the 2nd pressure vessel having same diameter as the first one. The figure shows the schematic of the absorber:

Figure 3. 7 Evaporator Coil

To achieve the cooling effect of 1-ton i.e., 3.5kW the length of the evaporator found to be is 10m but again the problem faced was space constraint and we also must place our absorber along with the evaporator in the 2nd pressure vessel, so instead of going with the approach of vertical or horizontal evaporators in conventional refrigeration system we make a 'coil type evaporator'.

The bending of 3/8 copper tubes is done using Spring Bender available at MRC, SMME. The desired output diameter of the copper tubes is achieved by using a specified diameter plastic pipe and bending is done on it.

It is quite clear in the figure attached above that there are three copper coils of diameters as 85.725mm, 109.525mm, and 144.992mm to obtain the required heat transfer in this component.

At the top of the 2nd pressure vessels there is a spray nozzle which spray the cold saturated water on the evaporator coils turning them into water vapors. Since there is vacuum present inside the pressure vessel so water vapors will spread in the whole vessels.

Absorber

The next component in our refrigeration system is absorber which is placed below the evaporator in the lower pressure vessel. Note that there will be absorber sheet of dimensions 740mm, 235mm and 30mm having the capacity of 5.2liters. The following figure shows the schematic of the absorber.

Figure 3. 8 Absorber heat exchanger

To get the calculated heat transfer of 4.25kW in our absorber the calculated length of copper tube is 8m, which is achieved as above.

Using copper tubing cutter, copper tube is cut into desired length and then using the copper fitting that is copper T's and elbows we have made our model of absorber which is placed below the absorber sheet.

Now the concentrated Li-Br solution which was left in the generator sheet will be moved to the absorber sheet, where the fine hole in the absorber sheet will cause the Li-Br to move down like the droplets shape and thus increasing the affinity of the Li-Br Solution to absorb more water in it and then the Li-Br water solution will fall down on these absorber coils where heat will be transferred to the water present inside the coils and hot water will leave the absorber coils outside the pressure vessels.

The Li-Br water solution will be accumulated below the absorber and at the surface of the pressure vessels, and from there it will be accumulated outside the pressure vessel as a hole is drilled in the pressure vessel and again this Li-Br water Solution will be pumped to the generator dish using a pump outside.

Calculations for Solar Collector:

For harnessing solar energy from the Sun, we have different options for solar collectors. Flat plate solar collector, parabolic trough solar collector, parabolic dish solar collector, Fresnel solar collector and evacuated tube solar collectors were under our consideration. But we opt for parabolic dish solar collector. The comparison of efficiencies of different solar collector are given in the following table:

Table 3. 3 Comparison of solar collectors [34]

Motion	Collector Type	Absorber Type	Concentration Ratio	Indictive Temperature Range (^{o}C)
Stationary	Evacuated tube collector	Flat	1	50-200
Single-axis tracking	Compound parabolic collector	Tubular	5-15	60-300
	Parabolic trough collector	Tubular	10-85	60-400
	Linear Fresnel reflector	Tubular	10-40	60-250
Two-axis tracking	Parabolic dish collector	Point	600-2000	100-1500

This shows that two-axis parabolic dish reflector is the best solution for us. As we need temperature between 100-110^{o}C for our generator and parabolic dish collector can give temperature above 100 degrees Celsius. And with the size big enough, it can give us the required mass flow rates for heat addition capacity of 5kW.

We found the figure of solar flux in 24 hours for winter and summer solace is for 35 latitudes. For Islamabad, latitude is 33.7, so we can have a good approximation.

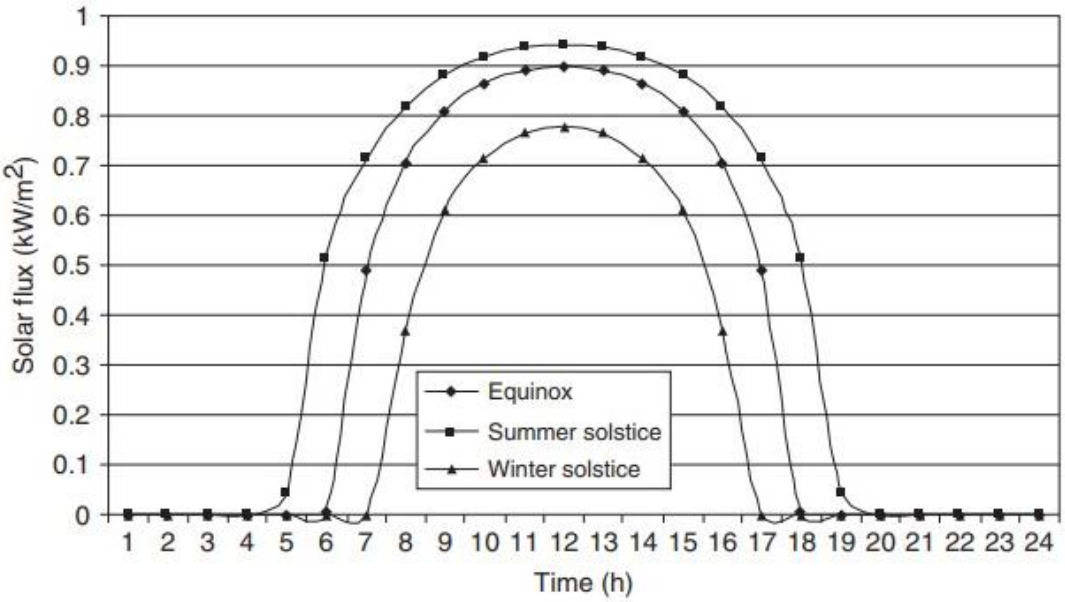

Figure 3. 9 Daily variation of solar flux [35]

We are going to use our refrigeration system in summers only for working hours from 9am to 5pm. So solar flux will remain above 0.8kW/m^2. We are using its value of 0.8 in our calculations as conservative approach.

For finding the area of solar collector, we use formula

Total rate of heat = Solar flux * efficiency of solar collector * Area of solar collector

$$Q_{collector} = \Phi * \eta * A$$

Since we need about 4.46 kW of heat in the generator, considering it to 5 kW as a conservative approach. Taking solar as 0.8kW/m^2 as discussed before and efficiency of solar collector as 0.8. The required area for the parabolic dish solar collector will be:

$$A = \frac{Q_{collector}}{\Phi * \eta} = \frac{5}{0.8 * 0.8} = 7.81 m^2$$

Now diameter of the dish:

$$d = \sqrt{4 * \frac{A}{\pi}} = 3.15m$$

By using the dish of diameter 3.15m, 1 ton refrigeration can be obtained.

Engineering Equation Solver Software:

We are currently working on the Engineering Equation Solver. It has a module for LiBr-H_2O solution vapor absorption cycle. Temperature-concentration-pressure and temperature-concentration-enthalpy values are stored in the software. By selecting the temperatures, software will give us the experimental values of concentrations and enthalpies. We have checked for each stage separately and our calculated values matched the values of the software. We are currently working on the complete code of EES.

CHAPTER 4: RESULTS AND DISCUSSIONS

To investigate the accuracy of the theoretical procedure described above in the chapter, a 4.46kW model was designed and will be constructed. All the calculations done in the above chapter assume of no energy losses and pure single state and the exit and entrance of each component. The design conditions of the chosen states are shown in the following table:

Table 4. 1 Water - LiBr absorption refrigeration system calculations based on a generator temperature of 90°C and absorber at 30°C

Point	h (kJ/Kg)	ṁ (kg/s)	P (kPa)	T (°C)	%LiBr (x)	Remarks
1	-168	0.006985	7.38	30	49	Weak solution at 30°C
2	-120.84	0.006985	7.38	50	49	Weak solution at 50 °C
3	-68	0.005485	7.38	90	62.4	Rich solution at 90 °C
4	-128	0.005485	1.23	60	62.4	Rich solution at 60 °C
5	2659.5	0.0015	7.38	90	0	Saturated water vapors at 90 °C
6	167.53	0.0015	7.38	40	0	Saturated water liquid at 40 °C
7	2519.2	0.0015	1.23	10	0	Saturated water vapors at 10 °C

We have stated all the parameters of our cycle that are calculated and shown in the last chapter. And remarks describe the state of each point according to figure 3.2.

Table 4. 2 Heat addition and rejection; COP of LiBr-H_2O cycle

Description	Symbol	kW
Cooling Capacity	$\dot{Q}_e$	3.5
Absorber Heat (Rejected to Environment)	$\dot{Q}_a$	4.25
Heat input to the Generator	$\dot{Q}_g$	4.46
Condenser Heat (Rejected to the Environment)	$\dot{Q}_c$	3.7
Coefficient of Performance	COP	**0.78**

0.78 COP means our cycle has the cooling capacity of 0.78 times the heat provided in the generator. It should be noted that we haven't include any heat losses and considered complete state change in the components. When practically system is running usually the fluid coming out of the component is not in pure vapor or liquid state. For example, after evaporator, refrigerant might have a bit of vapors in it. It means maximum possible cooling has not done in the evaporator. Similarly, heat losses through pipes and boundaries of components are also possible even after insulation. So usually, practical COP further reduces. One of the reports we found out stated the COP of 0.1 for 0.01 TR cooling capacity. It is significantly low than the theoretical COP of their cycle. The few reasons that they have low COP than the theoretical one is the size of system. For cooling capacity of 32W, a minute heat loss will incur a huge difference in COP. Atmospheric air is used to condense the refrigerant whose temperature may vary and can influence the generator pressure. By using water as a cooling fluid, we have a control on the condenser temperature. Proper cooling feed water supply to evaporator and condenser will improve

the efficiency of the cycle. 3 evacuated tubes are used of total effective area of 0.456m^2. This can be improved by using parabolic dish solar collector.

As already discussed, the pressure drop between evaporator and absorber has significant effect on the efficiency of absorption. In the discussed project, both evaporator and absorber are placed in a separate space which leads to pressure. We are going to place both components in a single vessel so the vapor drop between these components can be negligible.

We are keeping all these parameters into considerations and our designed system has these parameters into consideration, so it is expected to give higher COP than the discussed project. Once our fabrication is complete, we can verify this by experimentation.

We have a software code which can give the exact values for single stage of the cycle. This coding is done on EES and it takes initial temperatures and refrigeration capacity and give required heat and mass flow rates along with concentrations and enthalpies at each point. This code is the benchmark for our prototype, we can change the initial conditions and check how well our system is working. These experimental values can be used to optimize our working conditions and get better results.

the schematic diagram of our refrigeration system's mathematical model is shown below. Please note that all the notations in the coming graphs are made according to the schematic shown below.

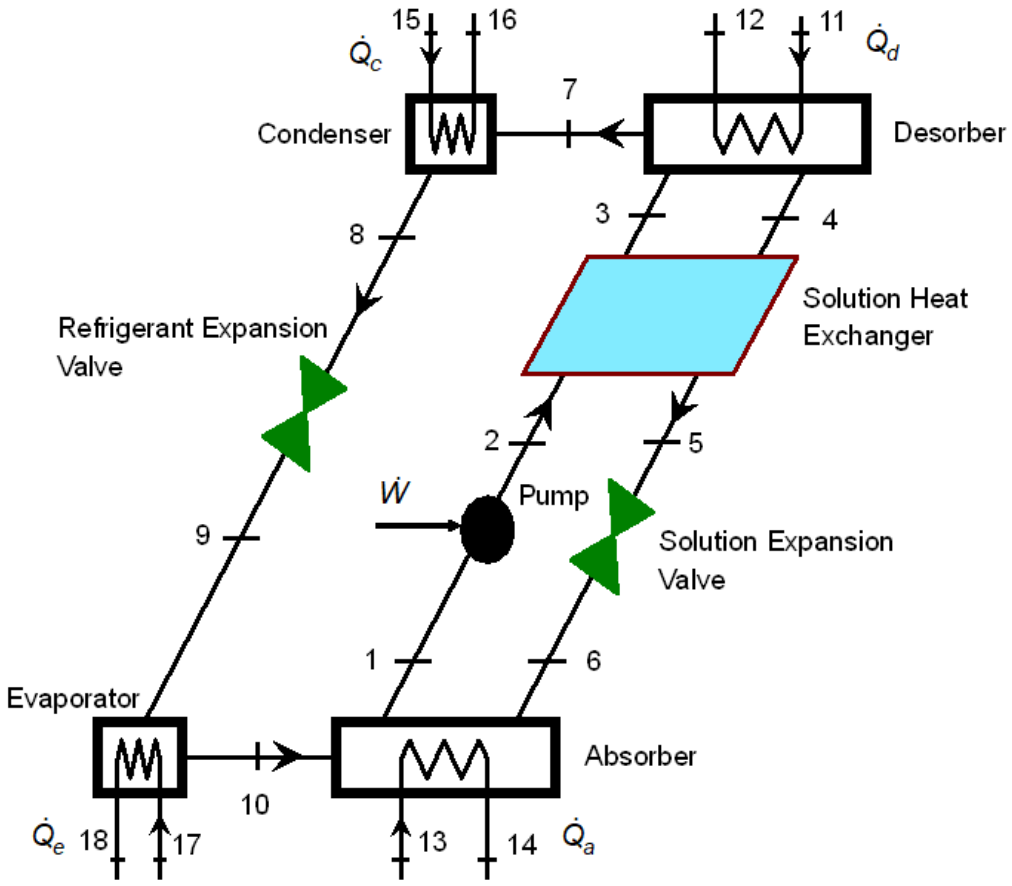

Figure 4. 1 Schematic for EES

Following results were obtained by running the mathematical model on software "Engineering Equation Solver".

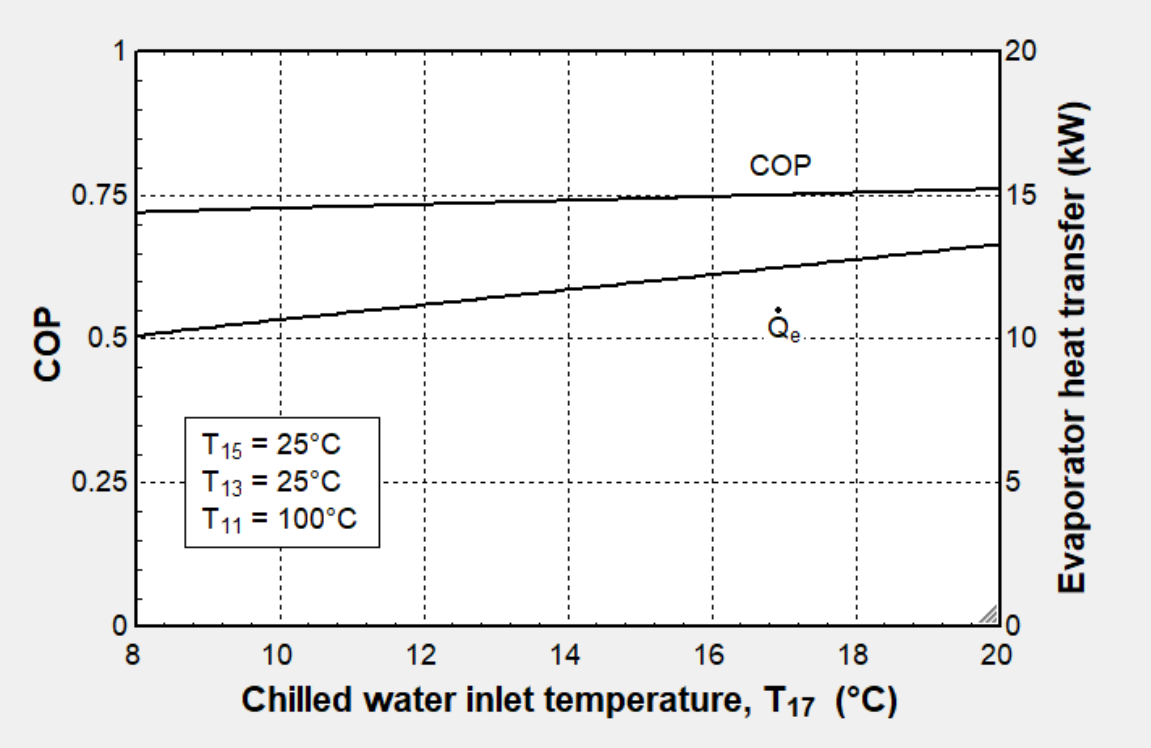

Figure 4. 2 Effect of chilled water inlet temperature at COP

Graph shows that as we increase the chilled water inlet temperature the COP as well as the heat transfer in our evaporator increases.

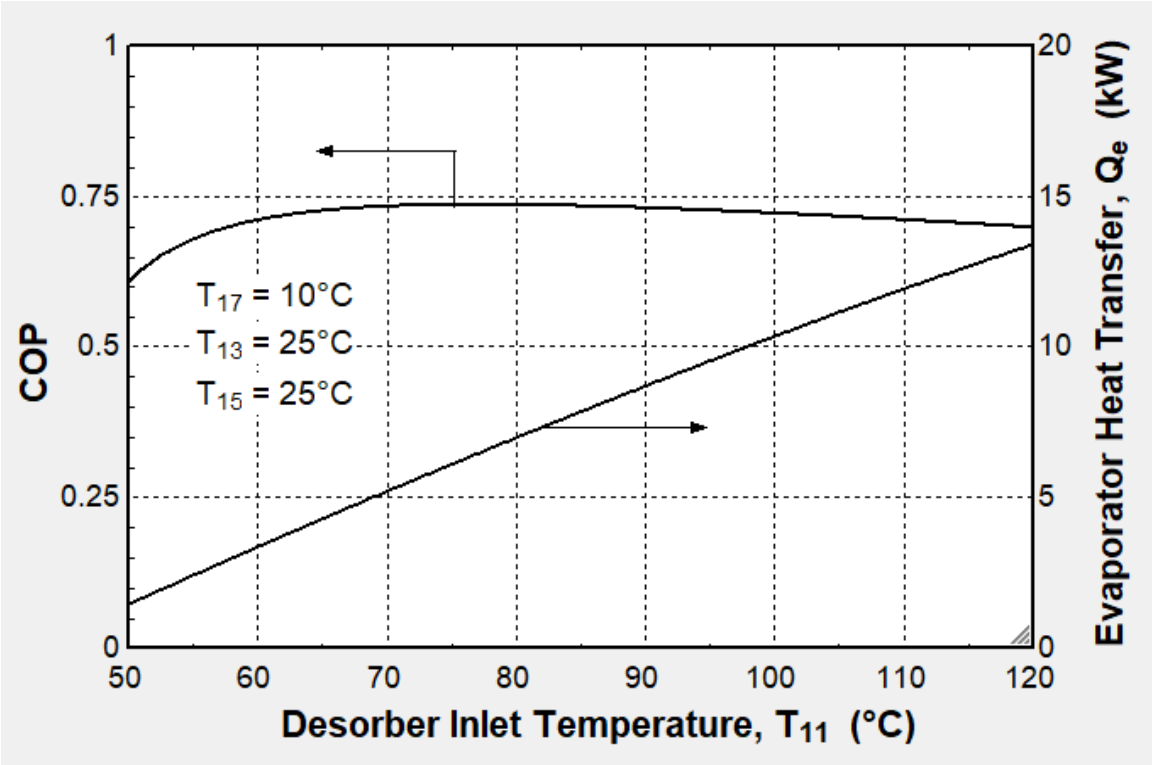

Figure 4. 3 Effect of desorber inlet temperature at COP

As the inlet temperature of our generator hot water increases the heat transfer in the evaporator also increases, but note that COP increases to a specified value of 0.74 at the temperature of 72^{o}C and then further increasing the generator inlet temperature decreases the overall COP.

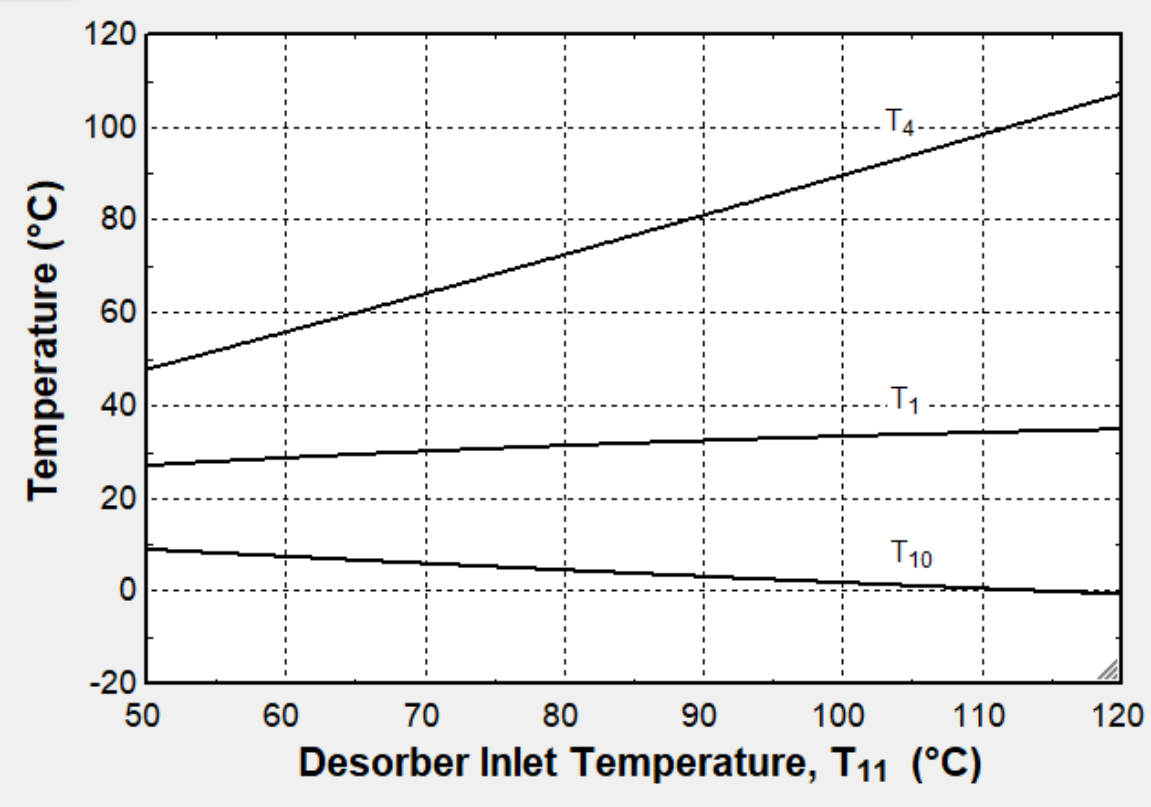

Figure 4. 4 Effect of desorber temperature

The above graph shows that as we increase the generator hot water inlet temperature the outlet temperature of strong LiBr Solution (T_4) increases but the outlet temperature of weak LiBr Solution(T_1) remains almost constant. On the other hand, the temperature of vapors going from evaporator to absorber(T_{10}) decreases.

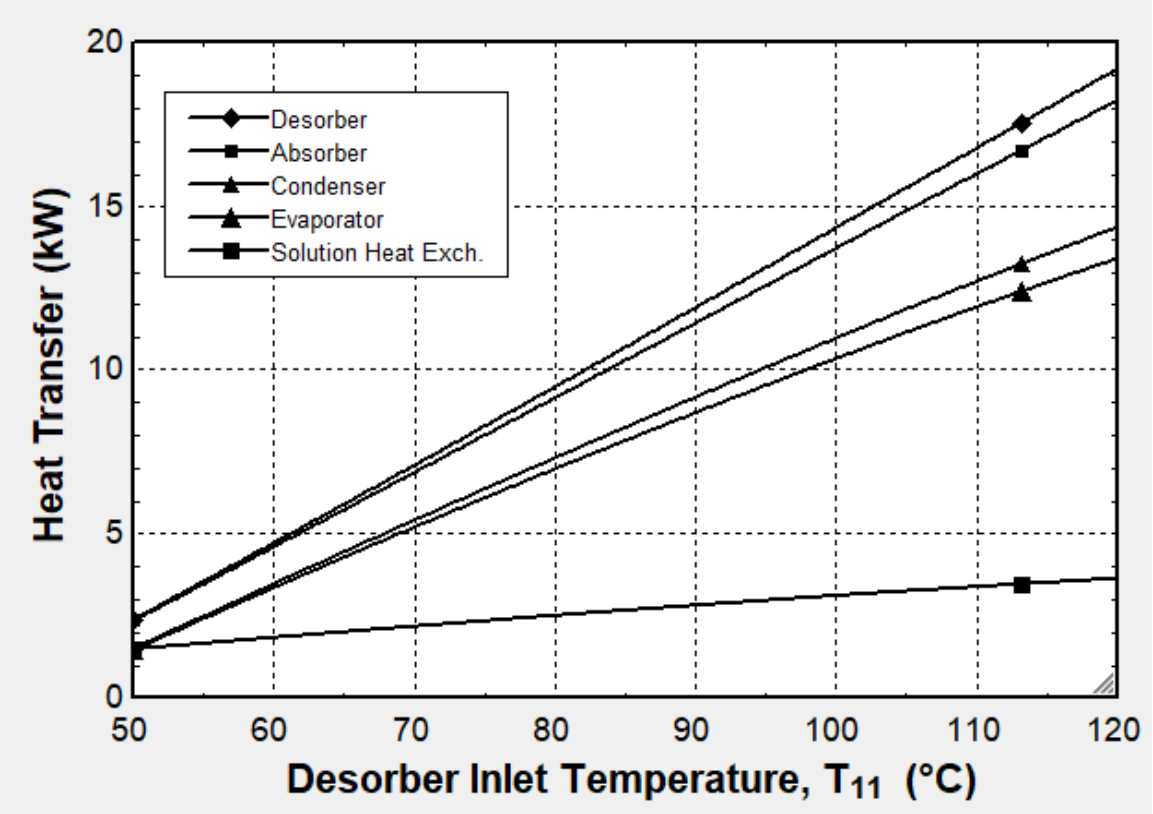

Figure 4. 5 Effect of inlet temperatures on heat transfer

It can be seen that as the temperature of generators hot water increases, heat transfer in all the components increases but heat transfer in heat exchanger of the weak and strong solution just slightly increases.

CHAPTER 5: CONCLUSION AND RECOMMENDATION

A vapor absorption refrigeration system is designed, with working fluid as LiBr-water and to be able to be powered by renewable and sustainable heat energy sources. However, we are going to power it by natural gas because due to budget and time limitation we could not go for solar collector and tracking system.

Based on our design system we are confident that this system can run on solar heat as a viable sustainable system as an alternative to the conventional refrigeration system. It can also be seen that this refrigeration system can be much more effective in the long run and since it requires heat energy as the input it can be used in remote areas as well with limited access to electricity. The unit proposes a strategy for providing maintenance free refrigeration to billions of people while also making a big contribution to curb climate change. Above literature has concentrated on the performance of the chiller and collector, but the next stage of development will almost certainly require additional attention to other system components as well as design, maintenance, and operation difficulties. As a result, the solar industry's challenge is to lower the total lifetime cost of solar-powered absorption chiller systems to improve the technology's economic viability, with the goal of eventually becoming competitive without subsidies.

REFERENCES

[1] A. A. A.-F. Nasiru I. Ibrahim, "Experimental investigation of a vapor compression system with condenser air pre-cooling by condensate," *Applied Thermal Engineering*, pp. 1255-1263, 2017.

[2] D. Y. G. Mehdi Zeyghami, "A review of solar thermo-mechanical refrigeration and cooling methods," *Renewable and Sustainable Energy Reviews*, vol. 51, no. 1364-0321, pp. 1428-1445, 2015.

[3] W. E. Resource, "World Energy Council," 2013. [Online]. Available: https://www.worldenergy.org/publications/entry/world-energy-resources-2013-survey.

[4] V. Bajpai, "Proceedings of the World Congress on Engineering," pp. 4-6, 2012.

[5] I. Horuz, "International Communications in Heat and Mass Transfer," pp. 25-711, 1998.

[6] J. H.-M. M. S.-R. a. W. R. L. Dominguez-Inzunza, "Applied Thermal Engineering," pp. 66-612, 2014.

[7] W. F. S. a. J. W. Jones, Refrigeration and Air conditioning, 2nd ed., pp. 333-334.

[8] W. F. S. a. J. W. Jones, Refrigeration and Air conditioning, 2nd ed., pp. 342-343.

[9] Y. A. Çengel, Heat and Mass Transfer, 4th ed., p. 441.

[10] Y. A. Çengel, Heat and Mass Transfer, 4th ed., pp. 441-442.

[11] M. Ozisik, Heat Transfer-A Basic Approach, McGraw-Hill Book Company, 1985.

[12] I. K. M. a. N. Morioka, *Absorption of Water Vapor into a Film of Aqueous Solution of LiBr Falling along a Vertical Pipe,* vol. 36, pp. 351-356, 1993.

[13] J. W. a. V. G. C. Andberg, "Design Guidelines for Water-Lithium Bromide Absorbers," *ASHRAE Trans,* vol. 89, pp. 220-232.

[14] S. Kalogirou, "Design and Construction of a Lithium Bromide Water Absorption Refrigerator," 2001.

[15] H. K. M. R. K. a. A. K. N. Varma, "Heat transfer during pool boiling of LiBr-water solutions at subatmospheric pressures. International Communications in Heat and Mass Transfer," vol. 21, pp. 539-548, 1994.

[16] H. K. M. R. K. a. A. K. N. Varma, "Heat transfer during pool boiling of LiBr-water solutions at subatmospheric pressures," *International Communications in Heat,* vol. 4, pp. 539-548.

[17] Y. A. Çengel, Heat and Mass Transfer, 4th ed., pp. 519-520.

[18] Y. A. Çengel, Heat and Mass Transfer, 4th ed., pp. 522-523.

[19] F. J. U. Jose Fernandez-Seara, "A general review of the Wilson plot method and its

modifications to determine convection coefficients in heat exchange devices," *International Communications in Heat and Mass Transfer.*

[20] F. J. U. Jose Fernandez-Seara, "A general review of the Wilson plot method and its modifications to determine convection coefficients in heat exchange devices," *International Communications in Heat and Mass Transfer.*

[21] "ASME Boiler and Pressure Vessel Code," *An international code,* 2010.

[22] Online. [Online]. Available: https://en.wikipedia.org/wiki/Renewable_energy.

[23] s. A. Kalogirou, "Solar Energy Engineering: Processes and Systems," 2nd ed., 2013, pp. 124-125.

[24] s. A. Kalogirou, "Solar Energy Engineering: Processes and Systems," 2nd ed., 2013, pp. 138-139.

[25] s. A. Kalogirou, "Solar Energy Engineering: Processes and Systems," 2nd ed., 2013, pp. 142-143.

[26] s. A. Kalogirou, "Solar Energy Engineering: Processes and Systems," 2nd ed., 2013, pp. 147-148.

[27] s. A. Kalogirou, "Solar Energy Engineering: Processes and Systems," 2nd ed., 2013, pp. 150-151.

[28] s. A. Kalogirou, "Solar Energy Engineering: Processes and Systems," 2nd ed., 2013,

pp. 151-152.

[29] s. A. Kalogirou, "Solar Energy Enigneering: Processes and Systems," 2nd ed., 2013, p. 126.

[30] S. A. S. M. Reyasudin Basir Khan, "Solar Tracking System Utilizing Pyranometer for Optimal Photovoltaic Module Positioning," *RimLife Greentech Technologies*, 2012.

[31] Y. L. Y. H. C. Han, "A Solar Ray Automatic Tracking Device Based on Image Sensor," *Chinese Control Conference*, pp. 5187-5190, 2011.

[32] G. V. A. Lay-Ekuakille, "PV Maximum Power Point Tracking Through Pyranometric Sensor: Modelling and Characterization," *Internatioal Journal on Smart Sensing and Intelligent Systems*, vol. 3, pp. 659-678, 2008.

[33] J. J. W.F. Stoecker, Refrigeration and Air Conditioning, 2nd ed.

[34] s. A. Kalogirou, "Solar Energy Engineering," 2nd ed., 2013, pp. 126-127.

[35] s. A. Kalogirou, "Solar Energy Engineering: Processes and Systems," 2nd ed., 2013, pp. 66-67.

[36] J. W. Jones and W. F. Stoecker, Refrigeration and Air conditioning, W. F. Stoecker, J. W. Jones, 2nd Edition, page # 332, Second ed., p. 332.

[37] W. F. Stoecker and J. W. Jones, Refrigeration and Air conditioning, Second ed., p.

335.

[38] [Online]. Available: https://en.wikipedia.org/wiki/Renewable_energy.

[39] [Online]. Available: https://en.wikipedia.org/wiki/Solar_panel.

[40] s. A. Kalogirou, "Solar Energy Engineering," 2nd, Ed., 2013, pp. 60-66.

[41] S. A. Kalogirou, "Solar Energy Engineering," 2nd ed., 2013, pp. 124-125.

APPENDIX I: TEMPERATURE-PRESSURE-CONCENTRATION GRAPH OF LITHIUM BROMIDE-H2O SOLUTIONS [36]

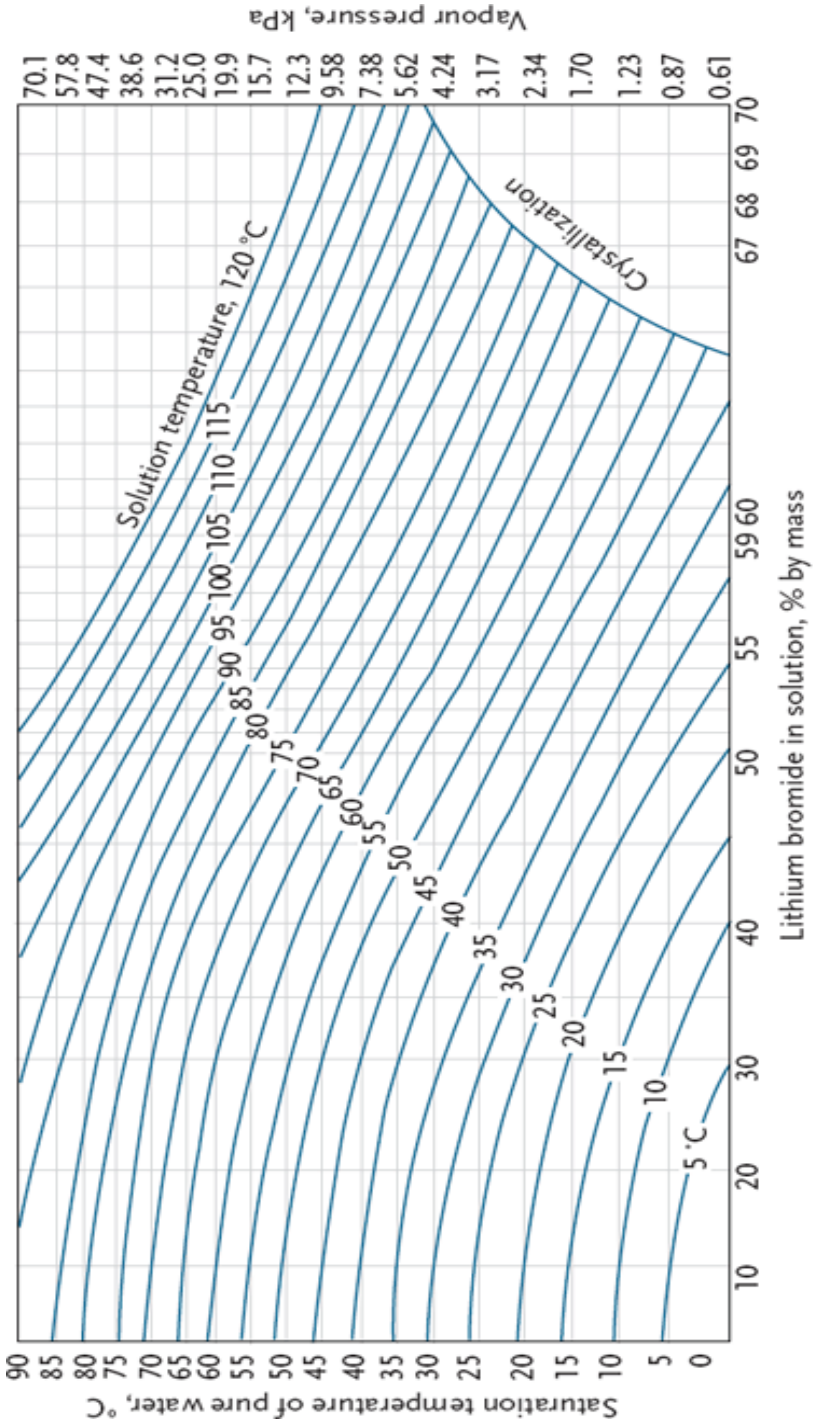

APPENDIX II: TEMPERATURE-CONCENTRATION-ENTHALPY GRAPH OF LITHIUM BROMIDE-H2O SOLUTIONS [37]

Please note that this graph is made according to reference stage of water property tables i.e., water has zero enthalpy at 0^{o}C.

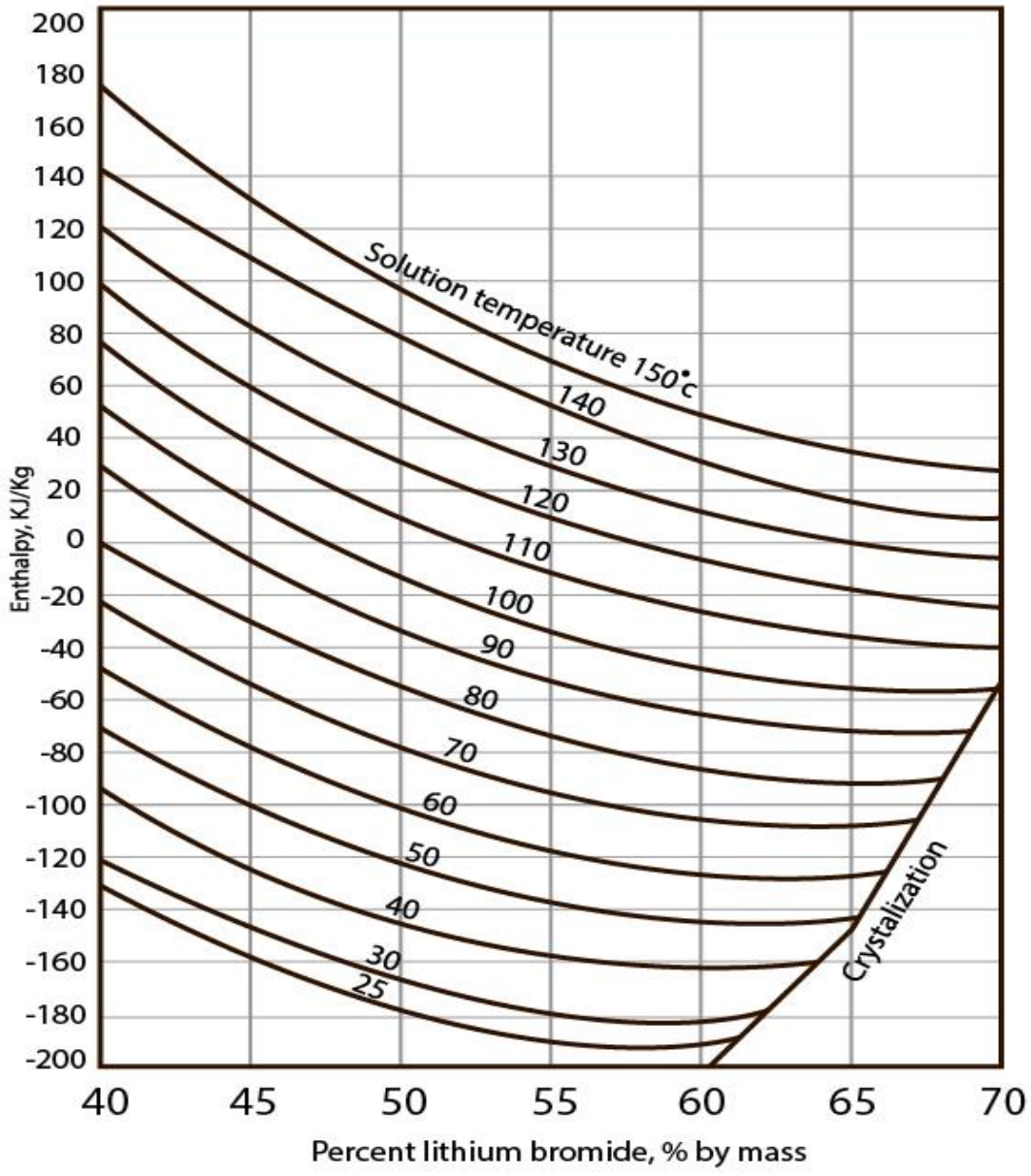

APPENDIX III: CACULATIONS

Enthalpy Calculation:

Mass flow rate of refrigerant

At stage 6:

h_6 = h of saturated liquid at T=40^{o}C → h_6 = 167.53 kJ/kg

At stage 7:

h_7 = h of saturated vapor at T=10^{o}C → h_7 = 2519.2 kJ/kg

$\dot{Q}_e$ = 1 ton = 3.5 kW

$$\dot{Q}_e = \dot{m}_5(h_7 - h_6)$$

3.5 = $\dot{m}_5$ (2519.2 – 167.53) → $\dot{m}_5 = \dot{m}_6 = \dot{m}_7$ = 0.0015 kg/s

Concentrations and other mass flow rates

Since generator and condenser are in same vessel, vapor pressure is equal in both components.

$P_g = P_{sat}$ of pure water at 40^{o}C → P_g = 7.38 kPa

For P_g = 7.38 kPa and T_g = 90^{o}C, from T-x-P graph for LiBr-H_2O solution

$x_3 = x_4$ = 62.4%

And,

Since evaporator and absorber are in same vessel, vapor pressure is equal in both components.

$P_a = P_{sat}$ of pure water at 10^oC → $P_a = 1.23$ kPa

For $P_a = 1.23$ kPa and $T_a = 30^oC$, from T-x-P graph for LiBr-H_2O solution

$$x_1 = x_2 = 49\%$$

Appling mass balance on absorber

Total mass balance:

$$\dot{m}_1 = \dot{m}_4 + \dot{m}_7 \rightarrow \dot{m}_1 = \dot{m}_4 + 0.0015 \quad (i)$$

Lithium bromide mass balance:

$$x_1\dot{m}_1 = x_4\dot{m}_4$$

$$0.49\dot{m}_1 = 0.624\dot{m}_4 \quad (ii)$$

By solving (i) and (ii) simultaneously, we get:

$$\dot{m}_2 = \dot{m}_1 = 0.006985 \text{ kg/s}$$

$$\dot{m}_3 = \dot{m}_4 = 0.005485 \text{ kg/s}$$

Enthalpies at unknown stages

At stage 5:

h_5 = h of saturated vapor at $T=40^oC$ → $h_6 = 2659.5$ kJ/kg

At stage 3:

For $P_g = 7.38$ kPa and $T_g = 90^oC$, from h-x-T graph of LiBr-H_2O solution

$$h_3 = -68 \text{ kJ/kg}$$

At stage 1:

For P_a = 1.23 kPa and T_a = 30^{o}C, from h-x-T graph of LiBr-H_2O solution

$$h_1 = -168 \text{ kJ/kg}$$

At stage 4:

The solution coming from the generator after passing through the heat exchanger is the stage at which crystallization is most likely to occur. We must keep its temperature high enough to avoid crystallization. From the graph, concentration = 62.4% and pressure of 7.38 kPa, we selected the minimum solution temperature as 60^{o}C.

For P_4 = 7.38 kPa and T_4 = 60^{o}C, from h-x-T graph of LiBr-H_2O solution

$$h_4 = -128 \text{ kJ/kg}$$

At stage 2:

For finding enthalpy at stage 2 we apply energy balance on heat exchanger,

$$\dot{m}_1(h_2 - h_1) = \dot{m}_3(h_3 - h_4)$$

$$h_2 = \frac{\dot{m}_3}{\dot{m}_1}(h_3 - h_4) + h_1$$

By substituting values, we get

$$h_2 = -120.84 \text{ kJ/kg}$$

From h-x-T graph of LiBr-H_2O solution,

$$T_2 = 50^oC$$

It shows that now solution enters the generator at 50^{o}C rather than at 30^{o}C (incase of without heat exchanger). This means less heat is required in the generator to get required refrigerant temperature and flow rate. It increases the efficiency of the cycle.

Heat addition in the generator

Apply energy balance on generator,

$$\dot{m}_2 h_2 + Q_g = \dot{m}_3 h_3 + \dot{m}_5 h_5$$

$$Q_g = \dot{m}_3 h_3 + \dot{m}_5 h_5 - \dot{m}_2 h_2$$

By substituting values, we get: $\dot{Q}_g = 4.46$ kW

Condenser

We need U for condenser:

$$U = \frac{1}{(D_0/D_i)(1/h_i) + (D_0/D_i)F_i + (1/2k)D_o \ln(D_0/D_i) + F_0 + 1/h_0}$$

$$D_0 = 9.525 \text{ mm} = 3/8''$$

$$D_i = 7.705 \text{ mm} = 1/3''$$

$$\frac{D_0}{D_i} = 1.236$$

k for copper tube $= 401 \text{ W}/mK$

Now

h_i (for cooling water)

Properties of water at avg. temperature $= \frac{40+30}{2} \Rightarrow 35°C$

$\rho = 994.08$ kg/m^3

$k = 0.6215$w/mK

$c_p = 4178$ J/kg°C

kinematic viscosity $v = 7.241 \times 10^{-7}$ m^2/s

$$\dot{m} = \frac{\dot{Q}}{c_p \Delta T} \Rightarrow \frac{3.7 \text{ kW}}{(4178)(10)} \Rightarrow 0.0885 \text{kg/s}$$

Now flow rate though copper tube:

$$Q = \frac{\dot{m}}{\rho} \text{ and } Q = Av \Rightarrow v = \frac{\dot{m}}{\rho \, . A}$$

$$v = \frac{0.0885}{(994.08)\left(\frac{\pi}{4}\right)(7.705 \times 10^{-3})^2}$$

$v = 1.91$ m/s

Reynold Number: $Re = \frac{v \, . \, D}{v} = \frac{(1.91)(7.705 \times 10^{-3})}{(7.241 \times 10^{-7})}$

$$\mathrm{Re} = 20{,}323.92$$

Prandtl No:

$$P_r = \frac{v.\rho.c_p}{k} \Rightarrow \frac{(7.241 \times 10^{-7})(994.08)(4178)}{0.6215} \Rightarrow 4.83$$

Nusselt $\mathrm{N_0}.\mathrm{N_u}: -$

From Heat and Mass Transfer Cengel for turbulent flow:

$$N_{\mathrm{u}} = \frac{(f/8)\mathrm{Re}\,\mathrm{Pr}}{1.07 + 12.7(f/8)^{0.5}(\mathrm{Pr}^{2/3} - 1)}\ , \qquad \begin{cases} 0.5 \le \mathrm{Pr} \le 2000 \\ 10^4 \le \mathrm{Re} \le 10^6 \end{cases}$$

Where Friction Factor: $f = (0.79\ln \mathrm{Re} - 1.64)^{-2}$, $10^4 \le \mathrm{Re} \le 10^6$

$$f = 0.026044$$

Now

$$\mathrm{N_u} = \frac{(0.026044/8)(20{,}324)(4.83)}{1.07 + 12.7(0.026044/8)^{0.5}(4.83^{2/3} - 1)} = 132.28$$

$$N_u = \frac{h_i\,.\,D_i}{k} \Rightarrow h_i = \frac{N_{\mathrm{u}} \cdot k}{D_i} = \frac{(132 \cdot 12)(0.6215)}{7.705 \times 10^{-3}}$$

$$h_i = 10670$$

And

h_o (for condensating refrigerant).

Nusselt's analysis of heat transfer for condensation on the outside surface of horizontal tube

$$h_m = 0.725\left[\frac{g\rho_l(\rho_l-\rho_v)h_{\mathrm{fg}}k_l^3}{\mu_l(T_v-T_w)D_0}\right]^{0.25}$$

Properties at average condensate film temperature $= \frac{40+30}{2} \Rightarrow 35^{\circ}\mathrm{C}$

$\rho_l = 994.08\ \mathrm{kg/m^3}$, $\rho_v = 0.03967\ \mathrm{kg/m^3}$

$h_{fg} = 2431.2\times10^3\ \frac{\mathrm{J}}{\mathrm{kg}}$, $k_l = 0.6215\ \mathrm{W/m^{\circ}C}$

$\mu_l = 7.191\times10^{-4}\ \frac{\mathrm{kg}}{\mathrm{ms}}$, $T_w = 30^{\circ}\mathrm{C}$

$T_v = 40^{\circ}\mathrm{C}$, $D_0 = 9.525\ \mathrm{mm}$

$h_m = h_0 = 12290.9\mathrm{W}/m^{2}{}^{\circ}\mathrm{C}$

Now $$U = \frac{1}{\frac{1.236}{10670}+\frac{1}{2(401)}(9.525\times10^{-3})\ln(1.236)+1/12290.9}$$

$$U = 5007.1\mathrm{W/m^2{}^{\circ}C}$$

Now for area of condenser:

ΔT_{i} = temp. at inlet $= 90 - 30 \Rightarrow 60°\mathrm{C}$

ΔT_0 = temp. at oullt. $\Rightarrow 42 - 40 \Rightarrow 2°\mathrm{C}$

$\mathrm{lm}td = \Delta T_{lm} = \frac{\Delta T_{\mathrm{l}} - \Delta T_0}{\ln\left(\frac{\Delta T_l}{\Delta T_0}\right)} \Rightarrow 4.72°\mathrm{C}$

$$\dot{Q} = \mathrm{U}.A.\Delta T_{\mathrm{lm}}$$

So, $$\mathrm{A} = \frac{3.7\ \mathrm{kW}}{(5000)(4.72)} \Rightarrow 0.156\ \mathrm{m}^2$$

Total area surface area $= 0.156\ \mathrm{m}^2$

The surface area of 1 m $3/8''$ pipe

$A = 2\pi r(1) \Rightarrow 2\pi(9.525 \times 10^{-3})$

$\mathrm{A} = 0.02999\ \mathrm{m}$

So, length of pipe

$$L = \frac{0.156}{0.02999} \Rightarrow 5.2\ \mathrm{m} \approx 6\ \mathrm{m}$$

Since h_m can be 20% higher or lower so 20% increase in length

$L = 7.75\ \mathrm{m} \approx 8\ \mathrm{m}$

so $L = 8\ \mathrm{m}$

Evaporator

Condensed refrigerant is getting sprayed on the evaporator coil. The heat transfer coefficient depends upon $\Delta T = T_{surface} - T_{boiling\ fluid}$. Since this temperature difference is about 25°C which is more than 10°C so nucleate boiling is taking place. The heat flux can be calculated by Rohsenow correlation.

$$\dot{q} = \mu_l h_{fg} \left[\frac{g(\rho_l - \rho_v)}{\sigma}\right]^{1/2} \left[\frac{C_p(T_s - T_{\text{sat}})}{C_{sf} h_{\text{fg}} Pr_l^n}\right]^3$$

μ_l at $T = 10°\text{C} = 0.0013076$ kg/ms

$h_{fg} = 2477.2 \times 10^3$ kJ/kg

$g = 9.8\ \text{m/s}^2$

$\rho_l = 999.75\ \text{kg/m}^3$

$\rho_v = \frac{1}{10632} = 9.405 \times 10^{-3}\text{kg/m}^3$

$\sigma = 7.42 \times 10^{-2}$ N/m

$T_s = 20°\text{C}$,

$T_{\text{sat}} = 10°\text{C}$

$C_{sf} = 0.0130$ $Ref.(P_g\#10$, MDPI Pool Boiling)

$P_{r_1} = 6.03$

$n = 1$ for water

$\dot{q} = 11.82\ (T_s - T_{\text{sat}})^3$

$\dot{q} = 11.82\ (10^3)$

$\dot{q} = 11.82$ k W/m^2

$\dot{Q}_e = 3.5\ kW$

$A = \frac{\dot{Q}_e}{\dot{q}} = \frac{3.5}{11.82} = 0.2961 \text{m}^2$

Surface Area of 1 m copper tube $= 3.14 * 9.5x10^{-3}$

$= 0.0298\ m^2$

To find the required length,

$$L = \frac{0.2961}{0.0298} = 9.9\ m \approx 10\ m$$

So, the length of evaporator tube is 10 m.

Vacuum Vessel

Fig CS-1 for factor B

B = From many charts depends on material type E

CS-1 – CS-6	Carbon Steel
HT-1 – HT-2	Low Alloy Steel

HA-1 – HT-10	Stainless Steel
CS-1 – CS-6	Carbon Steel
CT-1	Cast Iron
CD-1 – CD-2	Cast Ductile Iron

Calculations:

$$P = 0.1\text{MPa.}$$

$$T = 110°\text{C.}$$

$$D_0 = 26\text{mm} \qquad \because (22 + 4)$$

$$L = 1000 + 76\text{mm} = 1076\text{mm}$$

$$SS3041$$

Assume $t = 2\text{mm}$

$$L/D_o = 41.38$$

$$D_o/t = 13 > 10$$

ASME Sec. II DM Subpart 3 Fig. G, define 4D

Define A

Factor A for $(L/D_o = 41.38, D_o/t = 13 > 10)$

= 0.007

Interpolating value of E from fig. HA-3

For $T = 110°C$.

$$E = 187.06 \text{ x } 10^3 \, MPa$$

From figure CS-1,

B = 70 MPa

$$P_a = \frac{4B}{3(\frac{D_o}{t})}$$

$$P_a = \frac{4(70)}{3(13)}$$

$$P_a = 7.18 \, MPa$$

This is the maximum allowable pressure our vacuum vessel can handle on the outside but our vessel is working on atmospheric pressure so it is safe to use.